Argelander-
Institut
für
Astronomie

UNIVERSITÄT BONN
Rheinische
Friedrich-Wilhelms-
Universität Bonn

Models of massive binary star evolution as progenitors of gravitational wave events

Modelling a possible progenitor of GW151012 with ComBinE and MESA

Katharina Rauthmann

Masterarbeit in Astrophysik
angefertigt im Argelander-Institut für Astronomie

vorgelegt der
Mathematisch-Naturwissenschaftlichen Fakultät
der
Rheinischen Friedrich-Wilhelms-Universität Bonn

02.08.2021

I hereby declare that this thesis was formulated by myself and that no sources or tools other than those cited were used.

Bonn, 02.08.2021 Katharina Rauthmann

. . . . . .
Date

. . . . . .
Signature

1. Gutachter: Prof. Dr. Norbert Langer
2. Gutachter: Prof. Dr. Michael Kramer

Abstract

In 2015, LIGO and Virgo started a new era in astrophysics with the first direct detection of gravitational waves (GW). The detected events were produced by mergers of stellar black holes and neutron stars. In attempting to identify possible progenitor channels of double black hole mergers, we tap into the field of massive binary stellar evolution with many unsolved problems and which involves uncertain physics. Using the rapid binary evolution code ComBinE and the detailed stellar evolution code MESA, we investigate potential binary progenitors of GW151012, in which two black holes with masses of 23.3 and 13.6 solar masses merged. We identify the corresponding binary models, which we follow from zero-age main sequence through their supernovae and to the eventual GW merger.

We find that ComBinE predicts the existence of different binary formation channels that lead to a GW merger. For a range of initial orbital periods, the binary models are expected to undergo common envelope evolution, a process that is not yet well understood. As MESA can not routinely simulate the common envelope evolution or the impact of a supernova kick on a binary, we develop a method to calculate the consequences of these events from the detailed stellar models. We compare a ComBinE and a MESA model, which are created with significantly different methods but have similar outcomes. The MESA model predicts the common envelope ejection to be easier than was expected from the ComBinE results, which hints to an underestimate of merger rates for binary black holes in ComBinE. This strengthens the hypothesis that massive binaries contribute to double black hole mergers. We conclude that common envelope evolution is a viable pathway to produce gravitational wave events from massive binaries and that GW151012 can be explained by progenitors from this channel.

Acknowledgments

First and foremost, I want to thank Professor Norbert Langer, who has been the best supervisor I could ask for. His kindness and patience can not be overstated. Whenever I found it difficult to find my motivation, his enthusiasm about any new results helped me to go on. I would not have been able to complete this thesis were it not for him.
Secondly, I want to mention the members of the stellar evolution group, who always helped me find solutions to whatever questions I managed to come up with.
I also want to thank Professor Schmieden and Frau Zapf from the examination office for being so helpful and accommodating all this time.
Of course I would be remiss if I didn't also thank my partner, my family, and my friends. Their support was fundamental to my well-being and they gave me the will to carry on even when things got stressful and overwhelming.
Last but not least, my cat Annie, who has managed to be mental health support and constant distraction in equal measure. It is her you can think of when I use "we" or "our" in this thesis. She certainly has spent enough time sitting on documents and in front of the monitor.

Contents

Chapter 1

Introduction

For the entirety of human existence, light was the only way to investigate the universe. At first, people were limited to light visible to their eyes. More recently, they created telescopes for the entire spectrum of electromagnetic radiation. This limitation was finally overcome in 2015 when the first gravitational wave event was detected by LIGO and Virgo.

Gravitational waves are fundamentally different from light, as they are ripples in space-time itself. They were theorized in Einstein's theory of general relativity, and many cosmic events are predicted to produce gravitational waves of different frequencies.

LIGO and Virgo are able to detect a specific type of gravitational wave event, the merger of two compact objects. Compact object here refers to a stellar black hole, or a neutron star specifically, because detectors are not sensitive enough for mergers with a white dwarf yet. Neutron stars and black holes are the remnants of stars that were massive enough to end their life in supernovae.

The evolution of such massive stars is a field of active research, with many uncertainties and gaps in our knowledge. Thus, the detection of gravitational waves opens up a whole new avenue for examining the life of massive stars from the perspective of their eventual fate. How might the progenitors, which eventually merged in a gravitational wave event, have lived? What did they experience during their evolution? Did they spend their entire life together, or did they meet after their respective supernova? These are a few of the exciting questions for the field of stellar evolution. Such questions will probably accompany us for quite a while until they are solved. This thesis is supposed to be one piece of the large puzzle in front of us.

In this thesis specifically, we grapple with a central problem that poses itself when we try to explain how the progenitors of a gravitational wave event evolved as a binary. When two compact objects orbit each other, their orbital period slowly shrinks through the release of gravitational waves. This will eventually culminate in the detectable merger. However, slow in this case means on the order of the age of the universe. Therefore, for their merger to be observed today, the compact objects can not have been too far apart at their formation, only a few solar radii. But typically, massive stars expand to hundreds or even thousands of solar radii after exhausting hydrogen in their core. A binary of stars that started out close together would consequently merge during their evolution, and not get the chance to do so later as a gravitational wave merger.

To reconcile this contradiction, it has been suggested that the stellar components of the binary start out far apart. During their evolution, they interact, which results in a common envelope evolution. If the components survive this process, a very tight binary is created, which can eventually end in a gravitational wave merger if nothing else destroys it. This idea has been established as the standard formation channel for gravitational wave progenitors.

In this thesis, we will analyze models of binary evolution in detail. The goal is to find out whether the standard formation channel could explain a specific gravitational wave event, named GW151012.

This chapter provides an overview on the evolution of massive stars in binaries, including the common envelope evolution. Section 1.1 will also explain the standard formation channel. Section 1.3 gives more detail on the aim of this thesis, and Section 1.4 outlines its structure.

Table 1.1: Abbreviations used throughout this thesis

Abbreviation	Meaning
BH	black hole
NS	neutron star
CE	common envelope
CEE	common envelope ejection
GW	gravitational wave (event)
RLO	Roche-lobe overflow (stable mass transfer)
SN	supernova
ZAMS	zero-age main sequence
He-star	helium star
SMC	Small Magellanic Cloud

1.1 Evolution of massive stars and their models

This section is a short overview about the evolution of massive stars, following the descriptions in Kippenhahn et al. (2012) and Langer (2012). Massive stars are those stars that end their life in a supernova, which generally creates either a neutron star or a black hole. For single stars, this is the case for initial masses $\gtrsim 8\,\mathrm{M}_\odot$. During their main sequence, they burn (fuse) hydrogen to helium in a convective core, which is surrounded by a radiative, hydrogen-rich envelope. After central hydrogen burning ends, which is the end of the main sequence, the core contracts and the envelope expands rapidly, transforming the star into a red giant. The envelope also becomes convective. The central core grows in mass over time through hydrogen burning in a shell around it. It continues contracting until it is hot enough to ignite helium. Later burning stages, from carbon to silicon, are fundamentally similar, with each stage being shorter-lived than the one before.

Once an iron core has been formed, no more nuclear fusion is possible, and the massive star ends its life in a supernova. The type of supernova and its remnant depend on the star's mass. While supernovae are observationally classified into different types, it is difficult to determine the exact relations between the progenitor and the observational properties of a supernova. This is particularly true for black hole progenitors, for which far less observational constraints exist than for neutron stars, for which pulsar observations are available. Some massive stars might even avoid the supernova altogether and collapse directly into a black hole.

Creating models of the evolution of massive stars is difficult because many uncertainties about the processes underlying their evolution remain. One of the central problems is the treatment of internal mixing in massive stars, particularly mixing due to rotation, convection, including convective overshooting, and semiconvection. Semiconvection is especially problematic for models of massive stars, as it "is essentially unsolved" (Langer (2012), section 4.3.2). These processes are not the focus of this thesis, but as any differences in their treatment in stellar models can cause large consequences, it is essential to pay attention whether their treatment, and chosen parameter values, are the same when comparing different models of massive stars.

Another complication is how mass loss from massive stars changes with their mass and metallicity. Wind mass loss is less influential for less massive stars and for lower metallicities. Mass loss rates become both more significant and more uncertain for initial stellar masses $\gtrsim 60\,\mathrm{M}_\odot$, with these

very massive stars evolving close to the Eddington limit. As this thesis is restricted to a maximum mass of $60\,M_\odot$ at a low metallicity (see Chapter 2), this complication is not central to our stellar models but has to be taken into account when attempting to draw more general conclusions.
The central complication to the evolution of massive stars that is crucial in this thesis is binarity. It is thought that a large fraction of massive stars resides in binaries, with about three quarters of all O stars undergoing a strong binary interaction during their lifetime. Even outside of strong binary interactions like Roche-lobe overflow (see Section 1.1.1) or common envelope evolution (see Section 1.1.2), the evolution of a massive star in a binary is more complicated than that of a single star. The evolution can look significantly different due to binary specific effects like tidal interactions. Massive stars that have gained mass in a binary are also thought to be the most rapidly rotating stars.
In binaries, the impact of a supernova on the companion also needs to be taken into account. The questions of how much mass is ejected and whether the remnant receives a supernova kick at formation (e.g. Hills (1983)) have consequences on the remainder of the binary evolution. Potential outcomes range from a merger to the disruption of the binary system.
To summarize, there are still many things we don't know about the evolution of massive stars, which is especially true for binaries of massive stars. While this complicates determining the validity and applicability of a given binary star model, it also means that each new model can increase our knowledge about the evolution of massive stars.

1.1.1 Mass transfer

In a binary star system, the effective gravitational potential between the two stars has a surface passing through the equipotential Lagrange point, which is called the Roche lobe (e.g. Tauris & van den Heuvel (2006), which this section is based on). When one of the stars expands, it can fill its Roche lobe, initiating a mass transfer onto its companion, which is called the mass accretor or mass gainer. If this mass transfer is stable, the process is called Roche-lobe overflow (RLO). The stability of a mass transfer depends on the reaction of the star initiating Roche-lobe overflow (the mass donor) to losing mass and on the response of the Roche lobe.
The mass donor can react either through shrinking or expanding. If it expands, or the Roche lobe shrinks faster than the star does, the mass transfer destabilizes. Otherwise, the star remains within its Roche lobe and the mass transfer proceeds in a stable manner. For consequences of unstable mass transfer, see Section 1.1.2. According to Eggleton (1983), the Roche lobe can be approximated as a sphere with the so-called Roche-lobe radius

$$R_{\mathrm{RL}} = \frac{0.49q^{2/3}}{0.6q^{2/3} + \ln(1 + q^{1/3})} \cdot a\,, \tag{1.1}$$

where $q = m_{\mathrm{donor}}/m_{\mathrm{accretor}}$ is the mass ratio and a is the binary separation.
Depending on the evolutionary stage of the mass donor at the onset of a mass transfer, there are different cases of Roche-lobe overflow. In case A RLO, the mass donor is still on its main sequence, which means it is burning hydrogen in the core. Case B and C Roche-lobe overflow describe mass transfer after the main sequence, from a hydrogen shell-burning star or a helium shell-burning star, respectively. The mass gainer experiences spin-up from the accretion of angular momentum along with matter. This process needs to stop once the mass gainer reaches its critical rotation, the rotational velocity above which it would be torn apart. It is generally assumed that any accretion stops once the mass gainer reaches critical rotation, with the remainder of the matter leaving the mass donor being lost to the binary system. Due to mediation by tidal interactions, spin-up is weaker in very close binaries than in wide binaries.
Accretion can also cause thermohaline mixing in the mass gainer (see section 4.3.3 in Langer (2012)), as the accreted matter often contains helium-rich matter, which has a larger mean molecular

weight than the surface. This causes an inversion of the mean molecular gradient, which destabilizes the affected layers. This type of mixing is a significant complication to the mass transfer process, particularly in close binaries, where the stability of a mass transfer also strongly depends on the reaction of the mass gainer.

1.1.2 Common envelope evolution

If mass transfer destabilizes, common envelope evolution is initiated, a process we have little knowledge of. For a detailed review, see Ivanova et al. (2013), which this section is based on. Unstable mass transfer can be caused by the mass donor expanding relative to its Roche lobe or by instabilities such as the Darwin instability (Darwin (1879)). Potentially, a mass gainer can also initiate a common envelope if the mass transfer rate is too large to be accreted and the system can not expel the mass quickly.
Common envelope evolution starts once the envelope of the mass donor engulfs its companion, causing a frictional drag force to act upon it as it moves through the envelope matter. This leads to a spiral-in towards the core of the mass donor. In this process, orbital energy is released and deposited into the envelope.
Should the orbital energy overcome the binding energy of the envelope E_{bind} before the core of the mass donor merges with its in-spiraling companion, the common envelope is ejected.
This process can be studied quantitatively, using the energy budget formalism

$$|E_{\mathrm{bind}}| \leq \alpha_{\mathrm{CE}} \cdot |\Delta E_{\mathrm{orb}}| \,. \tag{1.2}$$

$|\Delta E_{\mathrm{orb}}|$ is the difference between the initial and final orbital energy, calculated according to

$$\Delta E_{\mathrm{orb}} = -\frac{G m_{2,\,\mathrm{core}} m_1}{2a_f} + \frac{G m_2 m_1}{2a_i} \,, \tag{1.3}$$

where m_2 is the mass of the donor, $m_{2,\mathrm{core}}$ is its core mass, and m_1 is the mass of the in-spiraling companion. G is the gravitational constant, a_i is the initial binary separation at the onset of the common envelope evolution and a_f the final separation when the envelope is ejected.
The energy budget equation introduces the ejection efficiency parameter α_{CE}, to quantify which percentage of the released orbital energy can be converted into kinetic energy for the envelope.
The envelope binding energy consists of the gravitational binding energy and its internal thermodynamic energy U, written as

$$E_{\mathrm{bind}} = -\int_{m_{2,\,\mathrm{core}}}^{m_2} \frac{G m(r)}{r} dm + \int_{m_{2,\,\mathrm{core}}}^{m_2} U dm \,. \tag{1.4}$$

As of yet, it is unclear whether further energy terms would need to be included in the energy budget so that the calculation would be realistic.
In order to calculate the envelope binding energy, detailed models of the envelope structure are needed. To simplify the requirement, in particular for population studies, the (α, λ)-formalism was introduced, which approximates the envelope binding energy as

$$E_{\mathrm{bind}} = -\frac{G m_2 m_{2,\,\mathrm{env}}}{\lambda R} \,. \tag{1.5}$$

Here R is the radius of the mass donor prior to the onset of common envelope evolution, and $m_{2,\,\mathrm{env}} = m_2 - m_{2,\,\mathrm{core}}$ is its envelope mass. The parameter λ is an approximation for the structure of the envelope.

To determine the outcome of the common envelope evolution, the mass boundary between the core and envelope must be known, which constitutes a significant problem (Tauris & Dewi (2001)). If the envelope can be ejected, a tight binary of the mass donor's core and its companion is formed. Otherwise, the components merge. The entirety of the common envelope evolution is thought to take place in a thousand years or less (Podsiadlowski (2001)).

1.2 Standard formation channel for GW progenitors

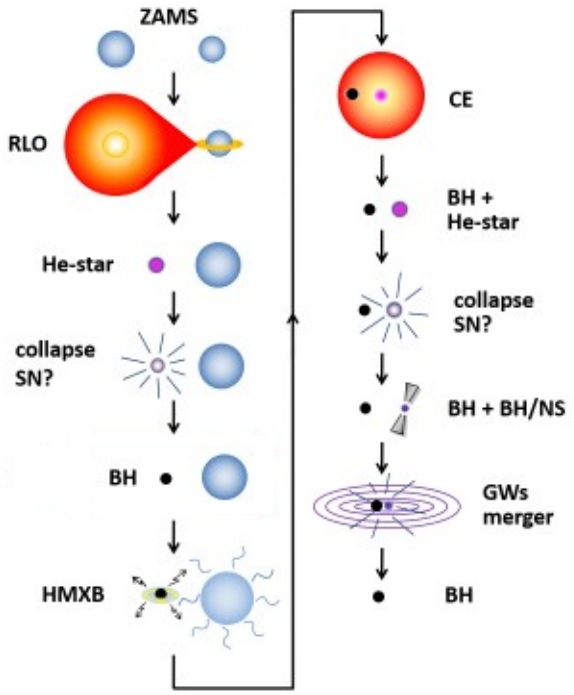

Figure 1.1: Representation of the standard formation channel for a massive star binary to a gravitational wave merger, including common envelope evolution. Adapted from Langer et al. (2020), originally from Kruckow et al. (2018). Abbreviations used: ZAMS: zero-age main sequence; RLO: Roche-lobe overflow; He-star: helium star; SN: supernova; BH: black hole; HMXB: high-mass X-ray binary; CE: common envelope (evolution); NS: neutron star; GWs: gravitational waves.

Over the last few years, a standard formation channel for the progenitors of binary black holes that end up merging in a gravitational wave event has been established (e.g. Belczynski et al. (2016), Kruckow et al. (2016), Stevenson et al. (2017)). The binary evolution following this formation channel is schematically shown in Figure 1.1. It starts with two massive zero-age main sequence stars. The initially more massive one is called the primary, the initially less massive one the secondary, this convention will be used throughout the thesis. The components start out far apart, with an initial orbital period on the order of years, but still close enough to interact at some point in their evolution.

Once the primary expands enough to fill its Roche lobe, with the timing dependent on the orbital period, stable mass transfer to the secondary is initiated. In this process, the primary loses its envelope, and the secondary gains mass (specifics see Section 1.1.1). When the binary detaches again, the primary has become a naked helium star.

The components continue their evolution separately, with the primary undergoing the post-main sequence burning phases and the secondary continuing on its main sequence with a larger mass

than before. Once the primary finishes fusing silicon into iron, it ends its life in a core collapse supernova and forms a black hole. The binary has entered the phase where it consists of a black hole and a main sequence star, during which it can become a high-mass X-ray binary (for research on this stage, see for example Tauris & van den Heuvel (2006), Langer et al. (2020)).

When the secondary leaves its main sequence, it rapidly expands to hundreds or even thousands of solar radii and its envelope becomes convective (Kippenhahn et al. (2012)). Therefore, when it fills its Roche lobe, the resulting mass transfer is destabilized, as the envelope responds to mass loss with further expansion (Tauris & van den Heuvel (2006)).

The envelope of the secondary engulfs its black hole companion, triggering the common envelope evolution. As the black hole moves through the envelope matter, a drag force is applied on the primary, causing a spiral-in towards the core of the secondary, releasing orbital energy in the process. If enough orbital energy can be deposited into the common envelope to overcome its binding energy before the black hole merges with the core of the secondary, the envelope is ejected from the binary. For more specifics about this process, see Section 1.1.2.

Surviving binaries are left with a small orbital period, on the order of hours. The core of the secondary continues its evolution as a naked helium star until it also ends in a supernova, forming a black hole or neutron star, depending on mass. The compact object binary is born. Its orbit shrinks through the release of gravitational waves, culminating in a merger, which can be observed as a gravitational wave event. Afterwards, a single black hole remains of the binary.

1.3 Aim of this thesis

The standard formation channel for gravitational wave progenitors has previously been investigated with rapid binary evolution codes. These codes are based on single star models and implement binary interactions in a simplified way. For the rapid binary code ComBinE, this method for binary star evolution will be discussed in detail in Section 2.1. With a rapid binary code, a large number of models can be evolved quickly, which is especially useful for parameter studies.

However, as discussed in this Chapter, binarity can affect the entire evolution of the binary's components, which the rapid binary codes can not include. Detailed stellar evolution codes solve the stellar structure equations for both binary components and can take binary specific effects, like tidal interactions, into account. Due to our lack of knowledge about the processes taking place during a supernova or a common envelope evolution, detailed stellar evolution codes can not routinely solve either of these events. Therefore, there is a distinct lack of detailed stellar models for the standard formation channel, which includes common envelope evolution. This thesis aims to change that.

While the detailed stellar code can not solve the impact of a supernova kick or the outcome of a common envelope evolution itself, the evolution of the binary before and after these events can be modelled in detail. Simplified calculations for the events can be implemented to connect the detailed models. In this way, we can effectively follow a binary model from the zero-age main sequence to the binary black hole phase and to the gravitational wave merger.

We start by finding potential progenitors for a specific gravitational wave event, using the rapid binary evolution code ComBinE. From the results, a promising progenitor model is chosen, and a comparable model with the detailed stellar evolution code MESA is created.

A fundamental question is whether the predictions from the rapid binary code still hold true for the presumably more accurate detailed model. The comparison between the predictions of the two types of binary evolution codes could tell us more about the feasibility of the standard formation channel. We also investigate whether previous studies might overestimate or underestimate the contribution of this formation channel to gravitational wave events.

1.4 Thesis structure

In Chapter 2, the methods we used for our investigation into gravitational wave progenitors are explained in detail. We also describe and justify our parameter choices.
Chapter 3 contains the results of our work. First, the models created with the rapid binary code ComBinE are investigated in detail. Each possible evolutionary path towards a gravitational wave merger is explained. In the second part of the chapter, the results from the model created with the detailed stellar evolution code MESA are analyzed. The model is compared to its equivalent ComBinE model.
The discussion of the results can be found in Chapter 4, which also contains an outlook towards possible future work on this topic.
Chapter 5 is the conclusion of this thesis.

Chapter 2

Methods and physical assumptions

In this chapter, the methods we used to find possible binary progenitors of gravitational wave events are explained.
The information we get from the detection of gravitational wave events is rather limited. In particular, a single event can be analyzed to provide ranges for the masses of the merging compact objects, sometimes a mass ratio, as well as peak luminosity, radiated energy, effective in-spiral spin, final spin and luminosity distance. By analyzing the frequency of detections, merger rates can also be inferred (Abbott et al. (2019)). But as discussed in the previous chapter, we know little about the progenitors that created the compact objects in the first place. To estimate a possible binary formation path for a double compact object merger, it is necessary to evolve a large number of binary system models. For this purpose, we use the rapid binary evolution code ComBinE, following the study by Kruckow et al. (2018) into several gravitational wave events. We restrict ourselves to a single gravitational wave merger, GW151012 (previously LVT151012), in order to study a possible formation path in more detail. The data about this event from LIGO is available in Table 2.1. GW151012 is one of the first three detections, which have been investigated for the longest time (e.g. Stevenson et al. (2017)). It is also particularly interesting because it potentially had an extreme mass ratio.
The speed of rapid binary evolution codes is their advantage in searching for possible progenitors of gravitational wave events, with the drawback of sacrificing the detailed models available in stellar evolution codes that solve stellar structure equations of both binary components.
To learn more about a possible progenitor model found with the rapid binary evolution code, we use the detailed one-dimensional stellar evolution code Modules for Experiments in Stellar Astrophysics (MESA). The key features of both codes will be explained in the following subsections.

Table 2.1: Observational data for GW151012 from LIGO (Abbott et al. (2019))

parameter	value
primary mass	$17.7 - 38.1\ M_\odot$
secondary mass	$8.8 - 17.7\ M_\odot$
final mass	$31.8 - 46.4\ M_\odot$
chirp mass	$14 - 17.3\ M_\odot$
mass ratio	$q \gtrsim 0.24$
peak luminosity	$84 - 220\ M_\odot c^2 s^{-1}$
radiated energy	$1.1 - 2.2\ M_\odot c^2$
effective in-spiral spin	$-0.15 - 0.36$
final spin	$0.56 - 0.8$
luminosity distance	$750 - 1400$ Mpc

2.1 ComBinE

We used the rapid binary evolution code ComBinE, a code for quick evolution of a large number of binary models with its origins in Tauris & Bailes (1996) and Voss & Tauris (2003). It was developed by Kruckow et al. (2018) and further modified by Christoph Schürmann (private communication). The basis of ComBinE are tabulated tracks from a grid of non-rotating single stellar models calculated with the detailed stellar evolution code BEC based on Brott et al. (2011), recreated by Kruckow et al. (2018) with mass ranges from 0.5 $M_\odot$ up to 100 $M_\odot$. For stellar models in between available tracks, values are interpolated. The binary interactions are calculated by ComBinE itself (see Section 2.1.3), after which components are attached to an appropriate single stellar model again. ComBinE computes only surface and core parameters (see Section 2.1.1 for specifics), there is no spatial separation for the models.
The BEC single star models include convection according to the standard mixing-length theory (Böhm-Vitense (1958)) with a mixing-length parameter of $\alpha_{\mathrm{MLT}} = 1.5$, using the Ledoux criterion to determine the boundaries of convective zones. Convective overshooting is included with a parameter $\alpha_{\mathrm{OV}} = 0.335$, as calibrated in Brott et al. (2011). Semiconvection, a process in superadiabatic layers stable according to the Ledoux criterion, is implemented based on Langer et al. (1983) with a semiconvection parameter of $\alpha_{\mathrm{SC}} = 1.0$ (Langer (1991)). Transport of angular momentum follows the description in Heger et al. (2000), including mixing due to rotationally induced instabilities, the dominant of which is the Eddington-Sweet circulation (Tassoul (1978)). More information on the effects of rotational instabilities is provided in Brott et al. (2011).
Mass loss from stellar winds follows the prescription by Yoon et al. (2006), which implements for surface helium mass fractions below $Y_{\mathrm{S}} = 0.4$ both the approach of Vink et al. (2001) and that of Nieuwenhuijzen & de Jager (1990), when the rate of wind mass loss calculated with the former prescription is lower than that of the latter approach. For hydrogen-poor stellar models ($Y_{\mathrm{S}} > 0.7$), the mass loss rate from Hamann et al. (1995) with a factor of 0.1 is implemented and an interpolation between the two is used for $0.4 \leq Y_{\mathrm{S}} \leq 0.7$. Brott et al. (2011) also includes rotational mass loss enhancement according to Yoon & Langer (2005).
Models were created by Kruckow et al. (2018) at four different metallicities, Milky Way (MW) at $Z = 0.0088$, Large Magellanic cloud (LMC) at $Z = 0.0047$, Small Magellanic cloud (SMC) at $Z = 0.0021$ and that of the dwarf galaxy I Zwicky 18 at $Z = 0.0002$.
As ComBinE assumes binary interactions to strip envelopes from mass donors, Kruckow et al. (2018) also created naked helium star models with the same stellar code, based on the isolated helium star models of Tauris et al. (2015). The same helium models are used for all metallicities in ComBinE, applying different mass loss rates scaled for metallicity.

2.1.1 Computed quantities in ComBinE

The ComBinE code can be used either for modelling one binary system with a more detailed output, or to create a large number of models. When one system is evolved, we can manually input the kick velocity w, as well as the kick angles θ and φ, or the values can be chosen randomly from the ranges given in population synthesis (see Table 2.2). ComBinE calculates the evolutionary phases a binary model goes through as explained in Section 2.1.3 and computes the following quantities for each phase and component: age t, mass m, radius R, luminosity L, effective temperature T_{eff}, and the envelope structure parameter λ for both components. Additionally, it keeps track of semi-major axis and eccentricity of the system. ComBinE also calculates galactic motion for the binary model, which is of no interest in this thesis and will not be discussed further.
When creating a large number of models, the ComBinE output for each binary model consists of initial and final values for the parameters mentioned above as well as a list of the evolutionary phases it went through.

2.1.2 Parameter choices

We chose to work with fixed initial masses at one metallicity for the binary in order to investigate the impact of other parameters. Previous studies have predicted that gravitational wave events and common envelope ejection are possible mostly at low metallicities (Kruckow et al. (2016), Kruckow et al. (2018) and references therein). Therefore, we chose to work with the metallicity of the Small Magellanic cloud (SMC). While an even lower metallicity (that of the dwarf galaxy I Zwicky 18) is available in ComBinE, our work in MESA is based on previous MESA studies (e.g. Marchant et al. (2016), Wang et al. (2020)), which were done with Z_{SMC} or higher metallicities.
For this thesis, we chose parameters within the ranges analyzed in Kruckow et al. (2018) (see table 2 therein for comparison with default ComBinE settings). For the chosen event GW151012 Kruckow et al. (2018) could estimate possible progenitor mass ranges for SMC metallicity among others (see figure 23 therein). Primary and secondary mass depend on each other and range from $\sim 50 - 100\,\mathrm{M}_\odot$ for the primary and $\sim 30 - 55\,\mathrm{M}_\odot$ for the secondary. In order to minimize inaccuracies from the ComBinE interpolation, masses corresponding exactly to available stellar tracks at SMC metallicity were used. $60.0\,\mathrm{M}_\odot$ and $40.0\,\mathrm{M}_\odot$ were available zero-age main sequence (ZAMS) tracks, which were chosen for the primary and secondary respectively. The distribution of initial values for the semi-major axis a is flat in the logarithm of orbital period ($\log_{10}(P)$), maintaining the default distribution in ComBinE in this work. Kruckow et al. (2018) estimated a possible range of $\sim 50 - 10000\,\mathrm{R}_\odot$ for the initial separation of the progenitor. As $10^4\,\mathrm{R}_\odot$ is the maximum initial separation investigated, we extend this range to $2 \times 10^4\,\mathrm{R}_\odot$. Chosen initial values for the binary models are outlined in Table 2.2.
From the results of these models, one binary was chosen to be used in the single system mode of ComBinE and compared with a MESA simulation. The parameter choices for this model are found in Table 3.1 and are explained in Section 3.2, as the choice of a system to explore further depends on the results regarding the models created with ComBinE. The input physics remain the same.

Table 2.2: Initial values and parameter choices made for modelling a large number of binary stars in ComBinE. Compare with table 2 in Kruckow et al. (2018).

name	value
number of simulated binaries, N	9.3×10^5
primary mass, $m_{1,\mathrm{ZAMS}}$	60.0
secondary mass, $m_{2,\mathrm{ZAMS}}$	40.0
semi-major axis, a	$50 - 20000\,\mathrm{R}_\odot$
eccentricity, e	0
metallicity, Z	$\mathrm{Z}_{\mathrm{SMC}} = 0.0021$
rotation, v_{rot}	$0\,\mathrm{km\,s^{-1}}$
wind mass loss during RLO, α_{RLO}	0.20
minimum mass ejection by accretor during RLO, β_{min}	0.75
circumbinary torus mass transfer during RLO, δ_{RLO}	0
circumbinary torus size during RLO, γ	2
CE efficiency parameter, α_{CE}	0.50
fraction of internal energy during CE, α_{th}	0.50
mass ratio limit for stable/unstable mass transfer, q_{limit}	2.5
kick velocity from SN, w	$0 - 200\,\mathrm{km\,s^{-1}}$

2.1.3 Treatment of evolutionary phases in ComBinE

This section is a summary of section 2.2 in Kruckow et al. (2018), explaining the concepts crucial to our work in more detail.

Wind mass loss

The evolution of the stellar components follows the stellar grids or their interpolated values. Orbital widening due to mass loss is calculated according to the equation

$$\frac{a}{a_0} = \frac{M_0}{M} \,, \tag{2.1}$$

where a is the semi-major axis, M the total model system mass and a_0, M_0 are their initial values prior to mass loss.

Roche-lobe overflow

When one component of the model fills its Roche lobe, the resulting mass transfer can be either stable or unstable, with the latter leading to a common envelope. ComBinE uses three criteria to decide which case occurs. The first is related to the mass ratio $q \equiv m_{\mathrm{donor}}/m_{\mathrm{accretor}}$ of the system, with a critical mass ratio $q_{\mathrm{limit}} = 2.5$, where mass transfer remains stable only if $q < q_{\mathrm{limit}}$ (see Kruckow et al. (2018) for justification of the specific value). The second criterion requires an orbital period of $\gtrsim 3$ days for massive OB-star models to avoid a Darwin instability (Darwin (1879)). Thirdly, massive stars are expected to develop convective envelopes (see Section 1), which destabilize mass transfer. ComBinE assumes that mass transfer from models of giant stars only remains stable if the convective envelope does not exceed 10% of the stellar mass.
If the mass transfer remains stable, a simplified mass transfer model from Tauris & van den Heuvel (2006) is used to calculate the orbital period and mass changes due to the Roche-lobe overflow. The equation for post-mass transfer orbital separation used in ComBinE,

$$\frac{a}{a_0} = \left(\frac{q}{q_0}\right)^{2\alpha_{\mathrm{RLO}}-2} \cdot \left(\frac{1+q}{1+q_0}\right)^{-1} \left(\frac{1+\epsilon q}{1+\epsilon q_0}\right)^{2\cdot\frac{\alpha_{\mathrm{RLO}}\epsilon^2+\beta_{\mathrm{RLO}}}{\epsilon(1-\epsilon)}+3} \,, \tag{2.2}$$

where $\epsilon \equiv 1 - \alpha_{\mathrm{RLO}} - \beta_{\mathrm{RLO}}$ is the accretion efficiency, keeps $\alpha_{\mathrm{RLO}} = 0.2$ and $\beta_{\mathrm{RLO}} = 0.75$ as constant parameters regardless of the donor model's evolution and the parameter δ is set to zero (omitted from the equation).
Roche-lobe overflow during the main sequence (case A) is treated differently from later mass transfer during later evolutionary changes (modification by Christoph Schürmann). It is a slow mass transfer taking place on its nuclear timescale (after a fast phase on the thermal timescale) mediated by tidal interactions. The further apart the two components are, the later the onset of case A mass transfer and less mass can be transferred.
When the Roche-lobe overflow takes place after the donor has left the main sequence, the donor is assumed to lose its entire envelope during mass transfer, which takes place on its thermal timescale. It is then left as either a naked helium star model with the former core mass as total mass and evolves following the helium stellar tracks. Alternatively, if the donor was already helium-rich, a naked core of carbon and heavier elements is left, which is assumed to terminate before it can interact further with the other component. The other stellar model can only accrete mass until the accreted orbital angular momentum causes it to reach critical momentum. After mass transfer, it is attached to a new evolutionary track depending on its core and total mass. Due to accreted hydrogen, it appears younger than it is and thus is attached to a younger stellar track.

In order to determine the core mass of the donor $m_{2,\mathrm{core}}$ and its envelope mass $m_{2,\mathrm{env}} = m_2 - m_{2,\mathrm{core}}$, the core-envelope boundary for the stellar model must be known, which is not easily determined (Tauris & Dewi (2001)). ComBinE uses the criterion that the core is the central mass which contains less than 10% hydrogen (mass fraction of $X = 0.1$) at the onset of mass transfer, from Dewi & Tauris (2000). This is one of several possible methods for locating the bifurcation point (see section 4.1 in Ivanova et al. (2013)).
The most massive helium stars are expected to develop inflated envelopes (Köhler et al. (2015), fig. 5 in Kruckow et al. (2018)). In this case, the envelope filling the Roche lobe does not trigger the mass transfer algorithms of ComBinE, which are only activated once the non-inflated part of the envelope reaches the Roche-lobe radius. The boundary between the two regions is applied according to Sanyal et al. (2015).

Common envelope evolution

Whenever any of the criteria for stable mass transfer is not fulfilled, ComBinE assumes the immediate formation of a common envelope. Whether the common envelope can be ejected is determined with the (α, λ)-formalism (see Section 1.1.2, Ivanova et al. (2013)) and an assumption for the ejection parameter of $\alpha_{\mathrm{CE}} = 0.5$. ComBinE gets values for the λ-parameter, which depend on mass and evolutionary status of the donor model (Kruckow et al. (2016)), for every time step from the underlying stellar grid data. The internal energy U is calculated following Han et al. (1995). The binding energy of the envelope is then given by Eq. 1.5. The envelope can only be ejected if the released orbital energy equals or is greater than the binding energy, resulting in $|E_{\mathrm{bind}}| \leq \alpha_{\mathrm{CE}}|E_{\mathrm{orb}}|$, with the change in orbital energy given by Eq. 1.3.
If the envelope can be ejected, the resulting binary separation a is calculated according to the equation

$$\frac{a}{a_0} = \frac{m_{2,\mathrm{core}}}{m_2}\left(1 + \frac{2}{\alpha_{\mathrm{CE}}\lambda}\cdot\frac{m_{2,\mathrm{env}}}{m_1}\cdot\frac{a_0}{R}\right)^{-1}, \tag{2.3}$$

where a_0 is the system's semi-major axis at onset of common envelope, m_1 is the mass of the engulfed component and R is the Roche-lobe radius of the donor model at the onset of common envelope evolution. Possible changes in the binary components during the common envelope evolution are disregarded, which is assumes to take place on a time scale of ≤ 1000 years (Podsiadlowski (2001)). The binary separation after common envelope ejection is used to determine further binary evolution of the model. If the envelope can not be ejected, a merger is assumed to take place.

Treatment of the supernovae

In this, we will only summarize how ComBinE treats the formation of black holes, as we are only modelling stars massive enough to end their life as these compact objects. See Kruckow et al. (2018) for further details on supernovae in ComBinE.
The black hole is assumed to be formed by the mass of the carbon-oxygen-core ($m_{\mathrm{CO-core}}$) of the stellar model, with an additional fallback mass of 80% of the helium envelope, if applicable. The final equation is

$$m_{\mathrm{BH}} = 0.8 \cdot (m_{\mathrm{CO-core}} + 0.8 m_{\mathrm{He-envelope}}), \tag{2.4}$$

with the resulting mass lowered by 20% to account for the release of gravitational binding energy. The role of supernova kicks in black hole formation is largely unknown (see discussion in Section 4.1.1). ComBinE uses a flat 3-dimensional distribution up to 200 km s^{-1} for the kick distribution, which is parameterized by the kick velocity w and the kick angles θ ($\in [0:180]^\circ$) and

φ ($\in [0:360]^\circ$). For single system evolution in ComBinE, these three parameters can be randomized, as they are in the mode for creating a large number of binary models, or they can be input manually.
In order to calculate the supernova effects on the binary model, it is assumed that the companion star is not affected by the impact of the ejected supernova shell and that the collapse is instantaneous compared with the orbital period $P_{\rm orb}$ (Tauris & Takens (1998)). As a consequence of the virial theorem, the system can only remain bound after supernova mass loss if it ejects less than half its total mass (Hills (1983)). If the binary model remains bound, ComBinE calculates the post-supernova semi-major axis according to Tauris & van den Heuvel (2006) as

$$\frac{a}{a_0} = \frac{1-(\Delta M/M_{\rm i})}{1-2(\Delta M/M_{\rm i})-(w/v_{\rm rel})^2-2\cos(\theta)\cdot(w/v_{\rm rel})}\,, \tag{2.5}$$

where $M_{\rm i} = M_{0,\,\rm i} + M_2$ is the pre-explosion mass of the binary, $\Delta M = M_{0,\,\rm i} - M_{\rm BH}$ the ejected shell mass, w the SN kick velocity and $v_{\rm rel} = (GM_{\rm i}/a_0)^{1/2}$ the orbital velocity of one component with respect to the other when $r = a_0$ in the pre-explosion binary. θ is the angle representing the direction of the kick compared to the orientation of the pre-supernova velocity. The eccentricity e after the supernova is

$$e = \sqrt{1+\frac{2E_{\rm orb}L_{\rm orb}^2}{\mu G^2 M_1^2 M_2^2}}\,, \tag{2.6}$$

with the orbital energy $E_{\rm orb} = -GM_1M_2/r + 1/2\mu v_{\rm rel}^2$, the orbital angular momentum $L_{\rm orb} = r\mu\sqrt{(v_{\rm rel}+w\cos\theta)^2+(w\sin\theta\sin\phi)^2}$ and the reduced mass of the system $\mu = M_1M_2/(M_1+M_2)$.

Circularization

It is assumed that eccentric orbits in close binaries circularize due to tidal friction prior to mass transfer (Sutantyo (1974)). This effect is calculated via angular momentum conservation to be

$$\frac{a}{a_0} = 1-e_0^2\,, \tag{2.7}$$

for a given eccentricity e_0. This circularization prior to any binary interactions is the reason why only binary models starting without any eccentricity were chosen, as any initially eccentric orbit can be represented by an equivalently closer model without initial eccentricity.

Gravitational wave radiation and merger

The orbits of double compact object binaries will shrink due to gravitational wave radiation (Peters (1964)). The delay time until an eventual merger depends on the component masses m_1 and m_2, the semi-major axis a_0 and eccentricity e_0 after the second supernova. It is calculated in ComBinE using the Peters (1964) prescription with the equation

$$t_{\rm merge} = \frac{15}{304}\frac{a_0^4c^5}{G^3m_1m_2M}\Xi(e_0)\,, \tag{2.8}$$

where $M = m_1 + m_2$ is the total system mass and $\Xi(e_0)$ is

$$\Xi(e_0) \equiv \left[\left(1-e_0^2\right)e_0^{-\frac{12}{19}}\left(1+\frac{121}{304}e_0^2\right)^{-\frac{870}{2299}}\right]^4\cdot\int_0^{e_0}\frac{e^{\frac{29}{19}}\left(1+\frac{121}{304}e^2\right)^{\frac{1181}{2299}}}{\left(1-e^2\right)^{\frac{3}{2}}}{\rm d}e\,. \tag{2.9}$$

2.2 MESA

For a closer study of a possible binary black hole progenitor model, we use the binary module of the detailed stellar evolution code Modules for Experiments in Stellar Astrophysics MESA (Paxton et al. (2011), Paxton et al. (2013), Paxton et al. (2015), Paxton et al. (2017)), version 10398. This code solves the time-dependent differential equations of stellar structure for both components simultaneously. The input physics for our MESA models are chosen to resemble those of the single stellar models ComBinE relies upon as closely as possible, modified by the contribution of the binary physics used in MESA. This is done following the prescription for the models of Marchant et al. (2016) and Wang et al. (2020), where more details can be found.

Accordingly, convection is also implemented following the standard mixing-length theory using the Ledoux criterion with $\alpha_{\mathrm{MLT}} = 1.5$. For helium burning stars with masses $\geq 13\,\mathrm{M}_{\odot}$, the "MLT++" method is implemented to avoid envelope inflation. Overshooting is implemented with step overshooting and a parameter value of $\alpha_{\mathrm{OV}} = 0.335$. Semiconvection follows the Langer et al. (1983) prescription with a value for the semiconvection parameter of $\alpha_{\mathrm{SC}} = 1.0$ (Langer (1991)). Rotationally induced mixing follows the description in Heger et al. (2000).

Custom opacity files[1] based on the opacity tables from OPAL (Iglesias & Rogers (1996)) are included. This is a difference to the BEC models from Kruckow et al. (2018). The implemented stellar wind prescription also follows Yoon et al. (2006), with rotationally enhanced winds based on Heger & Langer (2000).

MESA's binary module computes the evolution of both model components simultaneously with their orbital evolution. The rotation of both components is assumed to synchronize to the binary's orbital period at the start of the evolution and the effect of this spin-orbit coupling due to tidal interaction is implemented according to Detmers et al. (2008). This approach is justified because close binary systems are expected to quickly be tidally locked (de Mink et al. (2009)), which constitutes a difference to the ComBinE models, as only non-rotating stellar models from BEC are available for the code to work with.

When one of the components reaches its Roche-lobe radius (see Eq. 1.1), mass transfer is initiated. MESA contains several possibilities for treatment of mass transfer (Paxton et al. (2017)), called either explicit or implicit schemes, we use the latter for our models. Specifically, the mass transfer rate is set such that the stellar model always stays within its Roche lobe. The accretor can only gain mass from mass transfer until it reaches critical rotation. Consequently, the mass accretion rate is set such that the accretor always stays just below critical rotation.

Mass transfer can lead to thermohaline mixing, which occurs when regions have an outwards increasing mean molecular weight (Wellstein et al. (2001)). It is implemented with an efficiency parameter of $\alpha_{\mathrm{th}} = 1.0$.

MESA can only simulate stable Roche-lobe overflow (as of version 10398). In case of instabilities, such as overflow of the component's second Lagrange point or if a limit of $(R - R_{\mathrm{RL}})/R_{\mathrm{RL}} \geq 100.0$ is exceeded, the evolution is stopped and a merger is assumed[2]. Further input parameters are taken from the SMC grid by Chen Wang (see Wang et al. (2020) and PhD thesis, to be released), which is based on Marchant et al. (2016).

As of the version used, MESA can simulate neither the effects of a supernova on a binary nor common envelope evolution. Therefore we developed a method to calculate their effects on the binary, enabling a second MESA simulation of the post-CE binary, provided it survives both events. As the goal was comparability between the ComBinE and the MESA model, the same methods for SN and CE treatment had to be used.

[1] `https://github.com/orlox/mesa_input_data`

[2] set by MESA binary controls, see `http://mesa.sourceforge.net/docs/r10398/binary_controls_defaults.html`

To simplify understanding, our combination of two MESA models, the first from zero-age main sequence to onset of common envelope evolution and the second simulating the post-common envelope binary, connected by our additional code, is called "the MESA model".

2.2.1 Treatment of the primary supernova

When the primary (initially more massive) model component depletes helium, its evolution in MESA is stopped and replaced with a point mass. The orbital period is set to effectively infinity (10^{99} days), allowing the secondary model to continue its evolution as a single star until it depletes helium as well. This is used for calculations of later interactions (see next subsection). Helium depletion was chosen as the stopping point for modelling as MESA often has convergence issues for massive stellar models in later stages of evolution. This stopping point allows us to use the same approach for the supernova and remnant formation as ComBinE. We wrote a code for the evolutionary stages starting at the primary supernova until the common envelope, which is available online[3], to facilitate these calculations.
With the computed quantities in MESA from the primary's model at helium depletion, the remnant mass is calculated according to Equation 2.4. The post-supernova separation and eccentricity are calculated from Equations 2.5 and 2.6, using the same supernova kick velocity and angles from the ComBinE model we want to compare the MESA model to.

2.2.2 Post-supernova binary until common envelope evolution

After the primary supernova, there should be no binary interaction until the common envelope, provided it happens at all. The secondary can thus be modelled as a single star until that interaction, which can not be modelled with MESA. Therefore, no new binary run with the post-supernova separation should be necessary because the available data from the secondary is sufficient. As in ComBinE, we assume that the orbit should circularize prior to any interaction. For simplicity, we apply the correction from Equation 2.7 immediately to the post-supernova separation.
The code written for the calculation of the binary separation does not contain a correction for wind mass loss from the secondary, which would widen the orbit again. Instead, a constant binary separation is assumed until the possible common envelope.
The code compares the radius evolution of the secondary with its Roche-lobe radius, which is calculated according to Equation 1.1 for every time step of the secondary model after the supernova of the primary, using the remnant mass from Eq. 2.4. If and when the radius of the model reaches or exceeds the Roche-lobe radius, mass transfer is assumed to set in. To determine whether the mass transfer is stable or triggers a common envelope, we use the same three criteria as ComBinE (Section 2.1.3). These are the possibilities of a critical mass ratio of $q_{\text{limit}} \geq 2.5$, an orbital period ≤ 3 days, or a convective part of the envelope exceeding 10% of the stellar mass. If any of these criteria are fulfilled, the mass transfer is destabilized and a common envelope evolution is assumed to set in.

2.2.3 Common envelope evolution

The common envelope is assumed to resolve instantaneously, which is not realistic, but with a timescale of ≤ 1000 years (Podsiadlowski (2001)), the time it takes is insignificant compared to the timescale of the entire binary evolution. The code takes the MESA output from the first secondary model exceeding its Roche-lobe radius (Eq. 1.1), which determines the envelope binding energy according to Equation 1.4. The internal energy in the MESA model is calculated as described in Paxton et al. (2017) (section 8). Two different calculations for common envelope ejection are

[3] `https://github.com/k-rauth/master-thesis`

made. Firstly, an ejection efficiency parameter of $\alpha_{\mathrm{CE}} = 0.5$ is assumed for a result comparable with the ComBinE model. Using the criterion that the released orbital energy must at least be equal to the envelope binding energy ($|E_{\mathrm{bind}}| \leq \alpha_{\mathrm{CE}}|\Delta E_{\mathrm{orb}}|$, Eq. 1.2), the final binary separation a_{f} is calculated as

$$a_{\mathrm{f}} = G m_{2,\,\mathrm{core}} m_{1,\,\mathrm{rem}} \cdot \left(\frac{G m_2 m_{1,\,\mathrm{rem}}}{2 a_{\mathrm{i}}} - \frac{E_{\mathrm{bind}}}{\alpha_{\mathrm{CE}}} \right)^{-1} , \tag{2.10}$$

where $m_{1,\,\mathrm{rem}}$ is the remnant mass of the primary, m_2 is the total mass of the secondary with $m_{2,\,\mathrm{core}} = m_2 - m_{2,\,\mathrm{env}}$ its core mass and a_{i} is the binary separation at onset of common envelope. The result is compared with the Roche-lobe radius of the secondary's core (Eq. 1.1). If the binary separation is larger than the Roche-lobe radius, the envelope can be ejected and the detached binary survives, otherwise it is assumed to merge.
Secondly, we can determine the value for the ejection efficiency parameter for the minimum final separation, where the core radius of the secondary equals its Roche-lobe radius $R_{2,\,\mathrm{core}} = R_{\mathrm{RL}}$. This results in the equation

$$\alpha_{\mathrm{CE}} = E_{\mathrm{bind}} \cdot \left(-\frac{G m_{2,\,\mathrm{core}} m_{1,\,\mathrm{rem}}}{2 a_{\mathrm{f}}} + \frac{G m_2 m_{1,\,\mathrm{rem}}}{2 a_{\mathrm{i}}} \right)^{-1} , \tag{2.11}$$

with the final separation

$$a_{\mathrm{f}} = R_{2,\,\mathrm{core}} \cdot \frac{0.6 q^{2/3} + \ln(1 + q^{1/3})}{0.49 q^{2/3}} . \tag{2.12}$$

Both envelope binding energy and the released orbital energy depend strongly on the core-envelope boundary. As we want to compare our model with the ComBinE results, we used the same criterion (see Section 2.1.3) of $X = 0.1$ at the boundary between core and envelope.
We assume that the primary black hole can not accrete any of the envelope matter during common envelope.

2.2.4 Post-common envelope binary with MESA

In case our calculations predict a successful common envelope ejection, a new binary MESA model can be created for the binary to simulate its further evolution. To maintain comparability with the ComBinE model, we use the binary separation after common envelope calculated with an ejection efficiency parameter value of $\alpha_{\mathrm{CE}} = 0.5$. We also assume that the entire envelope is stripped, leaving a pure helium model and use a helium zero-age main sequence stellar model at SMC metallicity to approximate this. The companion is a black hole, which is represented by a point mass in MESA. All other parameters are kept identical to the first MESA run.
The binary is evolved until the secondary depletes its helium, followed by applying the same supernova treatment as described above. If the binary survives the supernova, now as a binary black hole system, the remnant masses m_1 and m_2, post-supernova separation a_0 and eccentricity e_0 are used to apply the Peters (1964) prescription (see Equations 2.8 and 2.9) in order to calculate the time until the model merges in a gravitational wave event.

Chapter 3

Results

3.1 Models of binary stars with ComBinE

We ran population synthesis with ComBinE for 930,000[1] binary systems with the initial parameters from Section 2.1.2. The potential outcomes for the binary evolution of our systems fall into three categories: disruption, e.g. by a supernova; early merger, e.g. in a common envelope; or surviving as a binary until both stars are compact objects. We are interested in the survivors that will eventually merge in a gravitational wave event.

About 67% of the modelled binaries are disrupted by one of the two supernova kicks that occur at the end of the component's stellar evolution. We know that the supernova disruptions are not from the mass ejection criterion, as the initial component masses are always the same. This means that after a specific type of interaction, the component masses are also identical. Another 8% of all models merge early, either during a common envelope evolution or as a consequence of a supernova kick, although the former is more common (58,594 CE mergers versus 14,276 SN mergers). In total, almost three quarters of all models in the sample are either destroyed or merge early.

In our sample, 233,100 of the modelled binaries survive until the gravitational wave merger ($\sim 25\%$ of all models), which are plotted in Figure 3.1 with their merger times versus their initial orbital period ($\log P_\mathrm{i}$). The colors indicate the evolutionary path each system took. In our models the components of a binary can have two interactions during their lifetimes. The first can occur before the supernova of the primary, where it can initiate mass transfer, which either results in a stable Roche-lobe overflow (RLO) or unstable mass transfer, a common envelope (CE, see Section 2.1.3 for stability criteria). The second interaction can occur between the supernovae of the primary and the secondary, with the same possibilities as described above. In general, there are more possibilities for binary interactions, such as overcontact (see Marchant et al. (2016)), reverse mass transfer, or another Roche-lobe overflow after a successful common envelope ejection, but this is not the case for our chosen initial masses of $60\,\mathrm{M}_\odot$ and $40\,\mathrm{M}_\odot$ and the range of initial orbital periods.

The type of interaction depends on the orbital period, as evidenced in Fig. 3.1. It is also possible for the components not to interact at all (called 'none') if the orbital period at the time is large enough. Not all combinations of (non-)interaction can precede a gravitational wave merger. In particular, a common envelope from the primary always leads to an early merger of the system according to our models.

Consequently, six evolutionary paths to a gravitational wave merger remain. The most common path in our models is the one where the binary undergoes two Roche-lobe overflows ('RLO+RLO'). It is possible from the closest separation modelled up to an initial orbital period of $\log P_\mathrm{i} \sim 3.5$.

[1] reason for this specific number is a bug in the ComBinE code that should not affect the results, see Appendix A.1

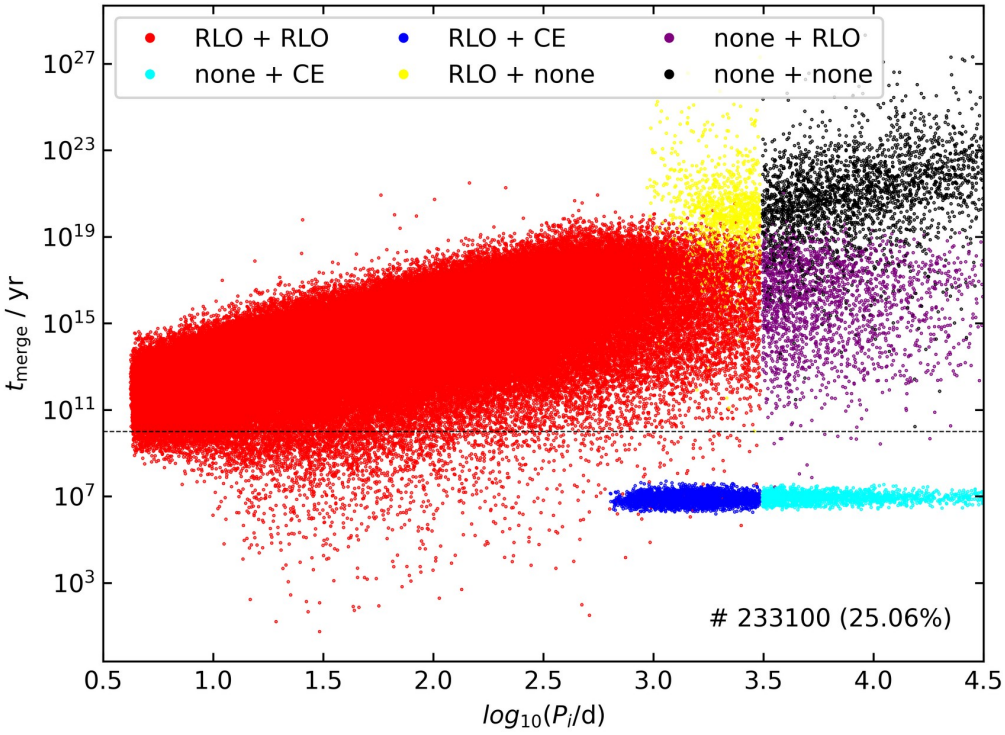

Figure 3.1: Gravitational wave merger times as a function of the initial orbital period for ComBinE models with specific initial masses, $60\,M_\odot + 40\,M_\odot$, with no initial eccentricity at SMC metallicity. In the bottom right, the total number of systems with an eventual GW merger is given, percentage of all simulated systems in brackets. The color-coding shows the different possibilities for first and second major interactions (see legend) that can lead to a GW merger. The first major interaction happens before the first supernova, the second interaction between the first and second SN. The dashed line indicates a merger time of 10^{10} years. Abbreviations used in this figure: RLO: Roche-lobe overflow; CE: common envelope; none: no interaction; interaction+interaction (e.g. RLO+RLO): interaction before the first supernova and interaction between first and second SN.

There is a strong divide at $\log P_\mathrm{i} \sim 3.5$ between systems experiencing Roche-lobe overflow in the first phase and those without interactions prior to the first supernova. This divide is a consequence of our assumptions of fixed masses and no initial eccentricity, which mean that any differences for systems with the same initial orbital period can only arise after the first supernova. For larger initial orbital periods, it is possible for binary models to not experience any interaction at all during their lifetime ('none+none').
If the first supernova kick tightened the binary enough for the components to interact, they can either undergo common envelope evolution ('none+CE') or stable Roche-lobe overflow ('none+RLO') with the secondary component as mass donor. The type of interaction depends on the orbital period after the supernova kick. If the components are close enough to interact before the secondary leaves its main sequence, a stable Roche-lobe will occur, as the critical mass ratio q_limit is never exceeded. An exception might be a rare case where the supernova kick decreases the orbital period to less than three days, which would trigger a Darwin instability. Presumably, such a kick would lead the

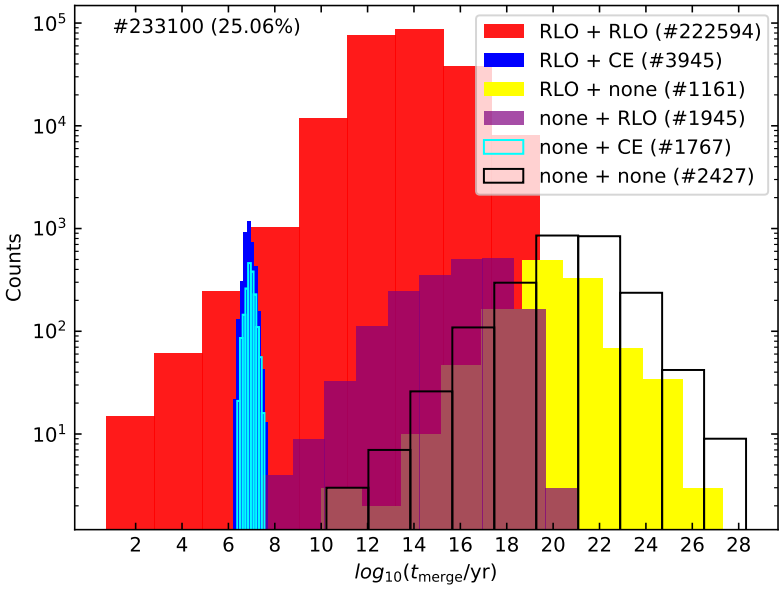

Figure 3.2: Histograms of the ComBinE systems in Fig. 3.1 showing counts of mergers at different times. Each histogram represents one of the six possibilities for major interactions and is color-coded (see legend). The legend also shows the number of binary systems evolving through each of the possibilities. The top left indicates the total number of systems with a GW merger. For abbreviations, see Table 1.1.

binary model to an early merger. On the other hand, if the orbital period of the binary model is large enough to trigger mass transfer after the secondary component has left its main sequence, it will result in a common envelope ('none+CE'). This is because the envelope of a massive star quickly becomes convective after hydrogen burning (see Kippenhahn et al. (2012), fig. 31.2), triggering the instability criterion in ComBinE.

The fifth possible evolutionary path for the models is the one where they undergo stable Roche-lobe overflow prior to the first supernova, followed by common envelope evolution thereafter ('RLO+CE'). This combination of major interactions is only possible for models with $2.8 \lesssim \log P_\mathrm{i} \lesssim 3.5$. The last of the six evolutionary paths occurs when, after a Roche-lobe overflow, the first supernova kick creates a binary separation too larger for further binary interactions to occur ('RLO+none'). This path is possible for initial orbital periods larger than $\log P_\mathrm{i} \sim 2.9$ and smaller than $\log P_\mathrm{i} \sim 3.5$.

As shown, each of the six possible paths to a gravitational wave merger covers a range of initial orbital periods with several of them overlapping. Apart from the fact that stable mass transfer or a common envelope are each possible across a range of separations, this is also due to the impact of the supernova kicks on the binary separation.

To get a better sense of the amount of models leading to a gravitational wave merger for the six evolutionary paths, Figure 3.2 shows a histogram for the number of models merging at different times. The color-coding for the evolutionary paths always remains the same. Only models with a merger time below $\sim 10^{10}$ years, which is roughly the Hubble time, predict a gravitational wave merger observable to us. This time is marked in Fig. 3.1. The histogram for all systems with a merger time below the Hubble time is shown in Figure 3.3, where the systems are sorted according to their initial orbital periods. Of the 233,100 models predicting the merger in a gravitational wave

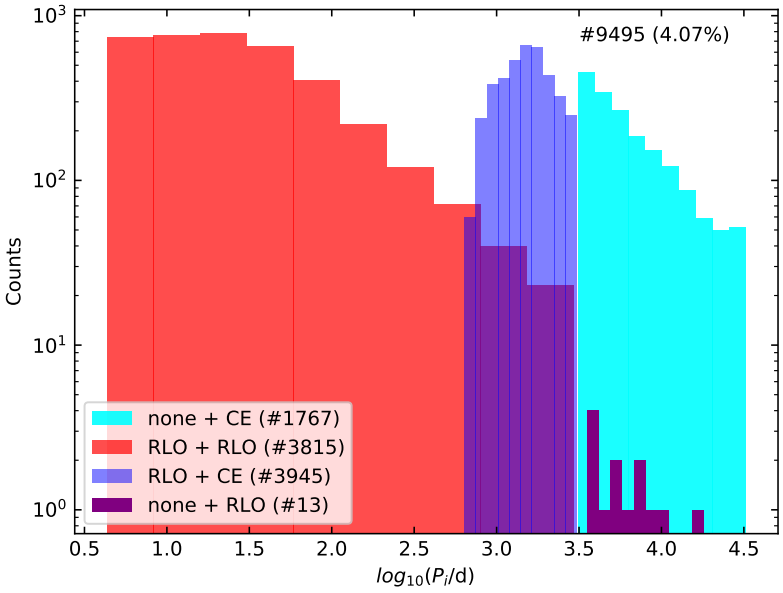

Figure 3.3: Histograms counting all ComBinE binary systems with a merger time below 10^{10} yrs, based on their initial orbital periods. The histograms represent the same systems with low merger times seen before (e.g. Fig. 3.4) and are color-coded according to the four possible variations of major interactions. The legend also shows the number of systems for each possibility. The top right shows the total number of systems with a GW merger within 10^{10} yrs, percentage of all models with a GW merger (regardless of merger time) in brackets. For abbreviations, see Table 1.1.

event, only 9,495 ($\sim$ 4%) would do so within 10^{10} years. Two of the six possible evolutionary paths don't produce any mergers within that time, as they result from systems that are too far apart after the first supernova to interact before the secondary ends its life. They are marked as 'RLO+none' and 'none+none'. The secondary kick, even when parameters align for strongest impact on orbital period, can not reduce it enough to create a merger within the Hubble time. These evolutionary paths are therefore of no further interest to us. The other four paths will be explained in more detail.

The vast majority of surviving models (222,594) go through two stable Roche-lobe overflows, the first one of which transfers mass from the primary component to the secondary (a main sequence star at that point). The second mass transfer occurs from the secondary component to the primary, the latter of which is a black hole at that point. Depending on the orbital period (initial or after the first supernova), the respective mass donor fills its Roche lobe either during its own main sequence (case A) or only after the main sequence, when its radius rapidly expands (case B). The type of Roche-lobe overflow also affects the final mass of the system, which will be explored further in Section 3.1.2. The large possible range for the supernova kick parameters (see Table 2.2) results in highly different orbital periods after the supernova, which creates differences in the evolutionary status of the secondary for the second Roche-lobe overflow. This is the case even for models with the same initial orbital periods. As the second supernova has a random kick as well, the models show a significant spread of orbital periods for the final binary black hole systems and therefore their merger times. Impact of supernova kicks for all evolutionary paths is explored further in Section 3.1.1. Most of the models have a merger time above $\sim 10^{10}$ years, which means their GW

mergers would not be observable today, if the models corresponded to real binary systems. Only about 3800 actually merge within that time ($\sim$ 1.7% of all surviving models with two RLOs).
The evolutionary path where the system undergoes a stable Roche-lobe overflow prior to the first supernova and a common envelope when the secondary expands during helium burning ('RLO+CE') corresponds to the standard channel for double compact object formation (Belczynski et al. (2016), see Section 1.1.2). All systems where the common envelope can be ejected develop into binary black hole systems that merge within the Hubble time (3945 systems). As Figures 3.1 and 3.2 show, there is indeed only a small spread in possible merger times, around 10^6 yrs $< t_{\mathrm{merge}} < 10^8$ yrs. This is a stark difference to the other evolutionary paths without a common envelope, which have a strong spread in merger times, most of which are larger than the Hubble time. Even though the vast majority of binary black hole mergers are created by two stable Roche-lobe overflows, there are more standard channel ('RLO+CE') mergers within the Hubble time than there are mergers from the former channel. This evolutionary path is not possible for models with $\log P_{\mathrm{i}} < 2.8$ because for these the first supernova kick can not increase the orbital period enough for the model to survive common envelope evolution. Survival is only possible for secondaries with a deep convective envelope, corresponding to a low binding energy (see Section 3.2.1 for more).
The third evolutionary path with a significant contribution to gravitational wave mergers within the Hubble time (1767 systems) is the one designated 'none+CE', i.e. the stellar models do not interact at all prior to the first supernova, which kicks the components close enough for a common envelope to form. Adding the number of models from both evolutionary paths containing common envelope evolution, a total of 5712 binary models with a common envelope successfully eject the envelope. On the other hand, 58,594 models merge during the common envelope. This means that only 11.3% of all binaries with common envelope evolution are predicted to survive it. ComBinE does not tell us in which part of a binary model's evolution the common envelope occurred, but a certain number of these models should have their common envelope evolution prior to the first supernova, which is always expected to end in a merger.
For an extremely small number of systems (13), the first supernova kick has parameters such that the orbital period after recircularisation is even smaller than for the 'none+CE' models and a stable Roche-lobe overflow can form ('none+RLO'). The kick from the secondary supernova results in a binary tight enough to merge within the Hubble time. Most of the systems following this evolutionary path (1945 in total) need much more than 10^{10} years to merge in a gravitational wave event. Due to the rarity of this path leading to an observable merger in these models, it is probably not a significant contributor to gravitational wave progenitors.
These results already hint that the exact properties of the supernova kicks play a crucial role in the evolutionary path a binary model will follow. Therefore, we take a closer look at their kick parameters and the consequences.

3.1.1 Supernova kicks

In this subsection, the impact of the supernova kick velocities and angles are explained for each of the four evolutionary paths with mergers within the Hubble time. As mentioned before, kick velocity is randomly chosen between $0 - 200\,\mathrm{km\,s^{-1}}$ for each supernova independently, the kick angles are randomly set for $\theta \in [0^\circ : 180^\circ]$ and $\varphi \in [0^\circ : 360^\circ]$. For any given initial orbital period, the primary supernova kick determines which evolutionary path a system takes through a change in orbital separation. Since the evolution of the systems was identical up to this point, the ejected mass is always the same. When the secondary supernova occurs, systems with the same initial separations can have had different interactions, which means that the ejected mass can differ as well. If the supernova kicks have a significant impact on the binary evolution, we expect the values to no longer be randomly distributed in our plots of surviving binaries, which are shown

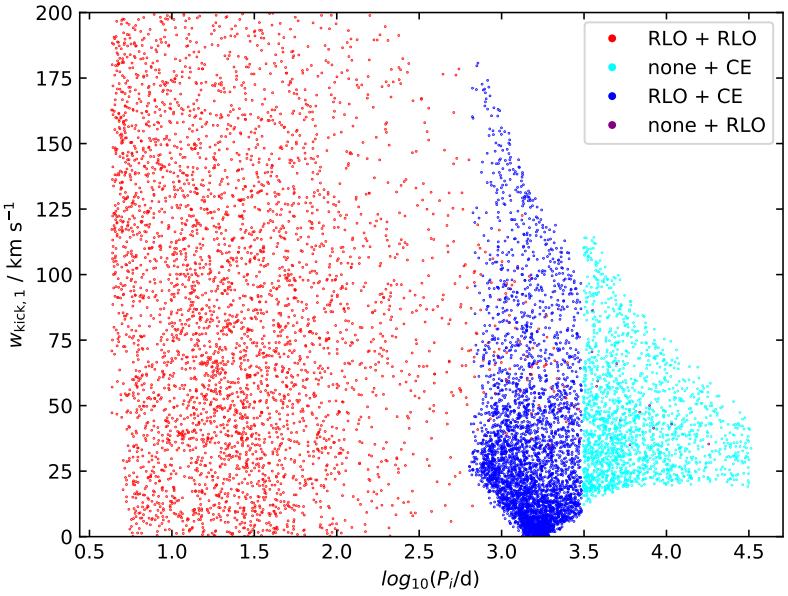

Figure 3.4: Kick velocities from the first SN for the ComBinE models from Fig. 3.1, which have a merger time below 10^{10} yrs plotted versus their initial orbital period. Color-coding (see legend) shows the four possible combinations of major interactions leading to a merger time within 10^{10} yrs. For abbreviations, see Table 1.1.

in Figures 3.4 to 3.9, where Figs. 3.4 - 3.6 are showing the parameters of the first supernova versus the initial orbital period for all systems merging within the Hubble time and Figs. 3.7 - 3.9 show the same for the second supernova. The exact merger time is not essential, as long as it is within 10^{10} years. In the Appendix A.2, the supernova parameters for all six evolutionary paths versus the merger time are shown as additional information.

RLO+RLO For the systems undergoing two stable Roche-lobe overflows, the velocity of the first kick appears to not be responsible for the outcome, as no velocity up to the modelled maximum of 200, km s^{-1} prevents a gravitational wave merger within the Hubble time on its own. An exception could be a few systems with the largest initial orbits ($2.5 \leq \log P_\mathrm{i} \leq 3.5$), but not enough models were created to identify a significant trend.
The same is true for the kick angle φ_1, while for the angle θ_1 there are some limitations for initially wide binaries (≥ 2.5), where θ_1 needs to be larger than $\sim 90°$, resulting in a binary separation that is decreased compared to its pre-supernova value (see Equation 2.5).
However, the supernova kick from the secondary component plays a crucial role for this evolutionary path. No system with a merger time below 10^{10} years has a secondary kick velocity smaller than $\sim 50\,\mathrm{km\,s^{-1}}$ and most of them even need a kick larger than $\sim 150\,\mathrm{km\,s^{-1}}$. The kick angle θ_2 needs values $\geq 120°$ and the second kick angle φ_2 mostly appears clustered around 0°, 180° and 360°, especially for larger initial periods, values at which the eccentricity is maximized through maximizing the orbital angular momentum L_orb (Equation 2.6).
From this follows that only a supernova kick which powerful enough and with aligned kick angles can bring the binary components close enough for a merger within the Hubble time. The precise binary evolution taking place before that second supernova is therefore not key to the outcome, including the first supernova. It mostly depends on the conditions of the secondary supernova kick

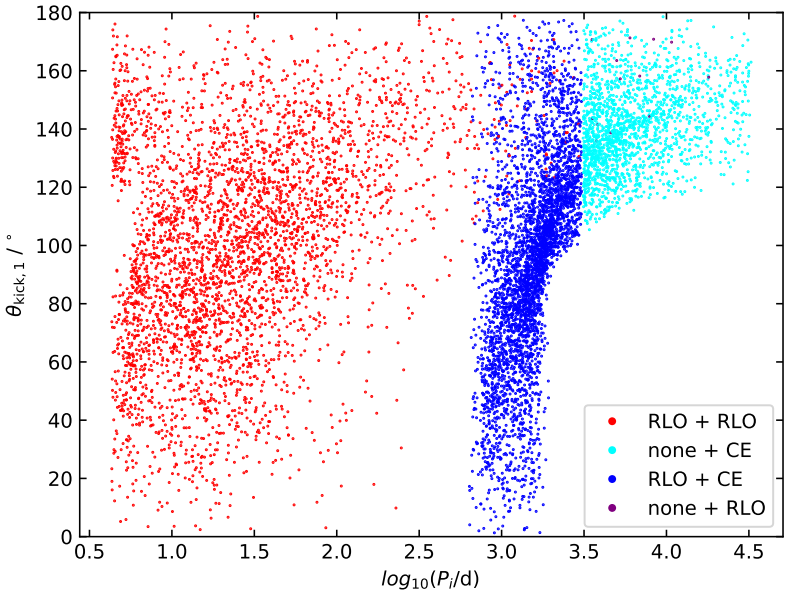

Figure 3.5: Kick angles θ from the first SN for the ComBinE models from Fig. 3.1 versus the logarithm of their initial orbital period. For each binary system, θ was randomly chosen between $0 - 180°$. Each of the four possibilities for major interactions leading to a GW merger within 10^{10} yrs are color-coded (see legend). For abbreviations, see Table 1.1.

being just right to create a black hole binary that is tight enough for an observable gravitational wave merger.

RLO+CE For the standard formation channel, it is the first supernova kick that determines much of the evolution, while the kick velocities and angles from the second supernova are irrelevant to the outcome. This is because a successful common envelope evolution creates a binary with a separation small enough to always merge within a Hubble time, which a supernova kick (at least up to 200 km s^{-1}) can not undo. This is why all binary models from the 'RLO+CE' evolutionary path fall within the Hubble time limit for the merger (see Fig. 3.1), the secondary supernova only creates some variation in the merger time. The first supernova kick on the other hand determines the orbital period of the binary and therefore whether a common envelope can form and the envelope can be ejected. The outcome for this evolutionary path mostly depends on the initial orbital period and the kick velocity from the first supernova.

Interestingly, it is the only channel that can produce any gravitational wave progenitors from our models without a supernova kick in either supernova nova, and only within a small range of initial orbital periods ($3.1 \lesssim \log P_\mathrm{i} \lesssim 3.3$, see Fig. 3.4). For all other initial orbital periods, at least a small supernova kick is needed, which increases the further the initial orbital period is from that range. There is also a maximum primary supernova kick velocity, above which the binary system follows another evolutionary path or is completely destroyed. The maximum velocity decreases with increasing initial separation, from ~ 180 km s^{-1} at $\log P_\mathrm{i} \sim 2.8$ to ~ 100 km s^{-1} at $\log P_\mathrm{i} \sim 3.5$. The supernova kick will also break the binary away from this evolutionary path for $\log P_\mathrm{i} \gtrsim 3.25$ if the kick angle θ_1 is too small (Fig. 3.6), as large values of θ decrease the binary separation (see Eq. 2.5). Otherwise, the kick angles are not relevant.

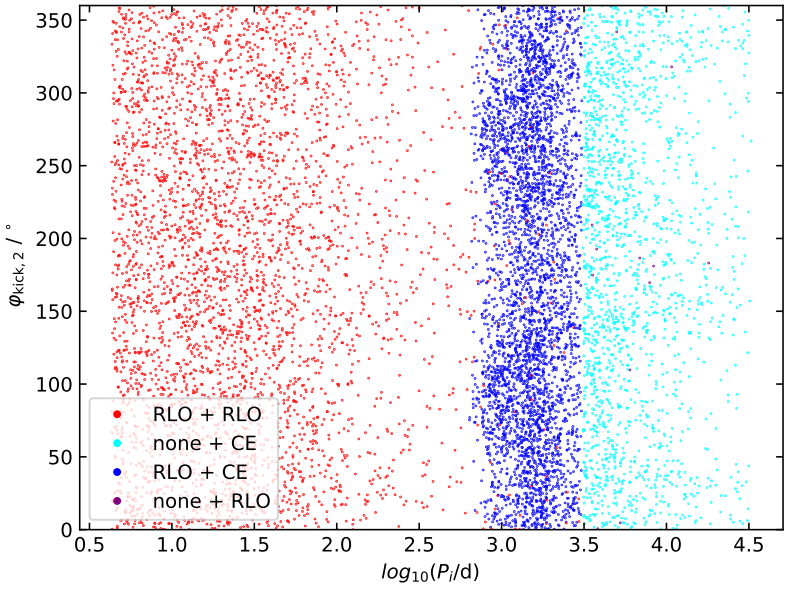

Figure 3.6: Kick angles φ from the first SN for the ComBinE models from Fig. 3.1 that merge within 10^{10} yrs versus the logarithm of their initial orbital period. φ was randomly chosen between $0 - 360°$ for each binary model. As before, major interactions are color-coded (see legend). For abbreviations, see Table 1.1.

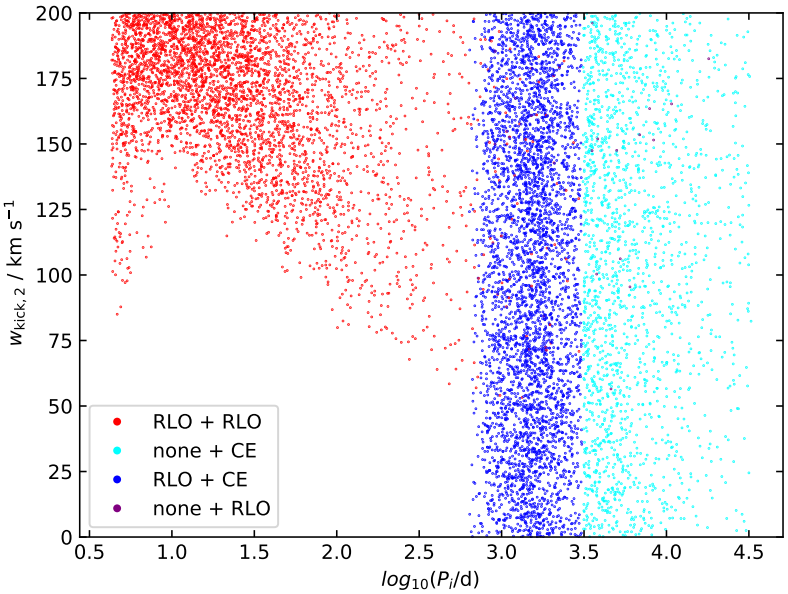

Figure 3.7: Kick velocities from the second SN for those of the ComBinE models which have a merger time below 10^{10} yrs plotted versus their initial orbital period. Color-coding (see legend) shows the four possible combinations of major interactions leading to a merger time within 10^{10} yrs. For abbreviations, see Table 1.1.

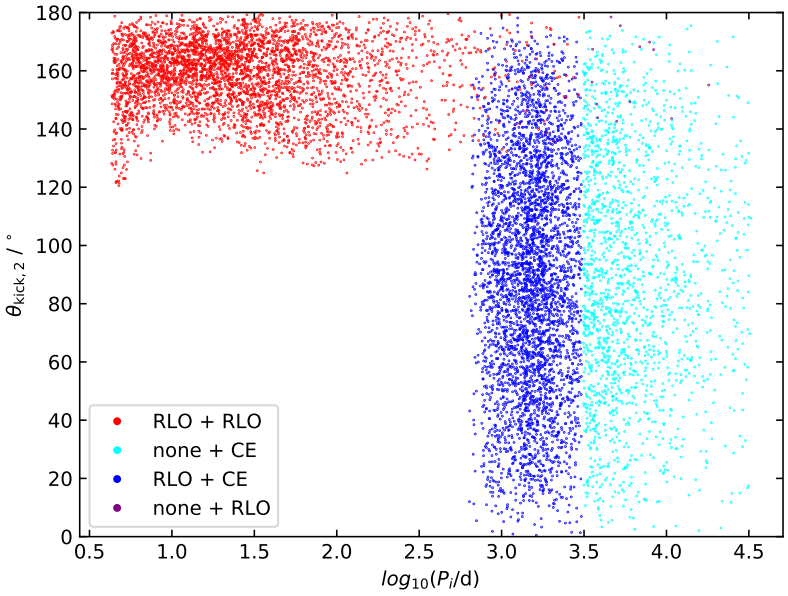

Figure 3.8: Kick angles θ from the second SN for the ComBinE models from Fig. 3.1 merging within 10^{10} yrs versus their initial orbital period. For each binary system, θ was randomly chosen between $0 - 180°$. Each of the four evolutionary paths leading to a GW merger within the Hubble time are color-coded (see legend). For abbreviations, see Table 1.1.

none+CE The conditions for the supernova kicks of the 'none+CE' evolutionary path are similar to those of the 'RLO+CE' path. As the outcome of the common envelope is the crucial factor for the final binary separation, the secondary supernova kick is not important. The constraints of the first supernova kick are more stringent than for the 'RLO+CE' channel however, as it is more difficult to create a system with the right separation for a successful common envelope if the initial orbital period was large enough for the components not to interact prior to the first supernova. At the same time, the kick velocity w_1 has to remain small enough not to break up the binary. The range for the first supernova kick velocity thus becomes smaller for larger the initial orbital separations, from $\Delta w = w_{1,\mathrm{max}} - w_{1,\mathrm{min}} \approx 100\,\mathrm{km\,s^{-1}}$ for $\log P_\mathrm{i} \sim 3.5$ to only $\Delta w \approx 30\,\mathrm{km\,s^{-1}}$ for the largest initial separation, $\log P_\mathrm{i} \sim 4.5$. The kick angle θ_1 also needs to have a value $\gtrsim 100°$ to ensure that the binary separation becomes smaller, with $\theta_{1,\mathrm{min}}$ increasing up to $\sim 120°$ for $\log P_\mathrm{i} \sim 4.5$. Models with even larger initial separations would probably still create this evolutionary path, with ever more narrow conditions on the supernova kick parameters, eventually requiring a highly eccentric orbit as well (through the kick angle φ_1, Fig. 3.6) to create the needed conditions.

none+RLO The contribution from this evolutionary path to systems with a merger time within 10^{10} years is with 13 systems ($\sim 0.7\%$ of all surviving 'none+RLO' systems) not large enough to give us statistically relevant information. From Figure 3.1 we can see that these systems are distributed through the entire range of this evolutionary path, with most of them falling just below the dividing line for the merger time. They are a product of the supernova kick parameters of both supernovae lining up just right to create a stable Roche-lobe overflow after the first supernova and to create a tight enough binary after the second. Therefore, this evolutionary path is exceedingly unlikely to make a meaningful contribution to observable gravitational wave mergers.

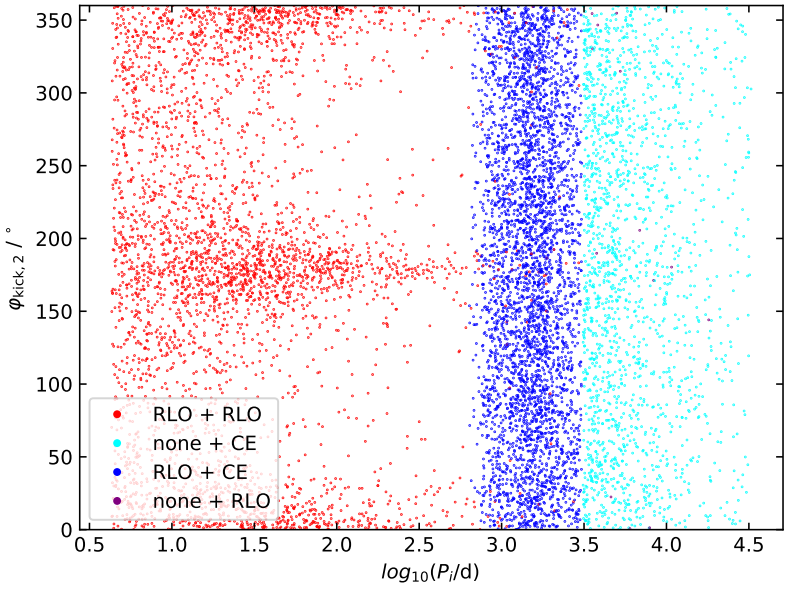

Figure 3.9: Kick angles φ from the second SN for the ComBinE models merging within 10^{10} yrs from Fig. 3.1 versus their initial orbital period. φ was randomly chosen between $0 - 360°$ for each binary model. As before, major interactions are color-coded (see legend). For abbreviations, see Table 1.1.

3.1.2 Final masses

Figures 3.10 and 3.11 show the final primary and secondary masses for each ComBinE model merging within a Hubble time, where the evolutionary paths are color-coded as before. Figure 3.12 shows the final total system mass for all these systems. Additionally, all three figures show the lower and upper bounds of the values for the event GW151012, as well as results from our MESA model, which will be discussed in Section 3.3. The final primary mass has a clear dependence on the initial orbital period with almost no variation at a specific value of $\log P_\mathrm{i}$ (Fig. 3.10). Up to an initial orbital period of $\log P_\mathrm{i} \sim 2.5$ ($P_\mathrm{i} \sim 316$ days), the final primary mass is larger the further apart the binary components started. For larger separations, the final primary mass stays the same, at $\sim 20\,\mathrm{M}_\odot$, regardless of the evolutionary paths the system took. All primary final masses are $> 15\,\mathrm{M}_\odot$ and therefore clearly black holes.

The evolution of the primary component in these models completely depends on the initial period - after it has become a black hole, only a small amount of additional matter can be accreted from the secondary component. The closest systems undergo case A Roche-lobe overflow (see Section 1.1.1) with the main sequence primary star as its mass donor. This type of mass transfer consists of two phases, a fast mass transfer on the thermal timescale, followed by a slow transfer on the nuclear timescale. The further apart the system initially is, the later the Roche lobe is filled and less mass can be transferred from the primary. For a comparison between systems undergoing case A mass transfer from the primary, see Figures 3.13 a)-c), where the effect on the primary mass can be clearly seen.

When the systems are far enough apart to initiate Roche-lobe overflow after the main sequence (case B), ComBinE handles the mass transfer always exactly the same (see Section 2.1.3): the entire hydrogen-rich envelope is removed and only a naked helium star remains, which then follows the prescribed helium star track. As the initial mass was identical, so is that of the helium core,

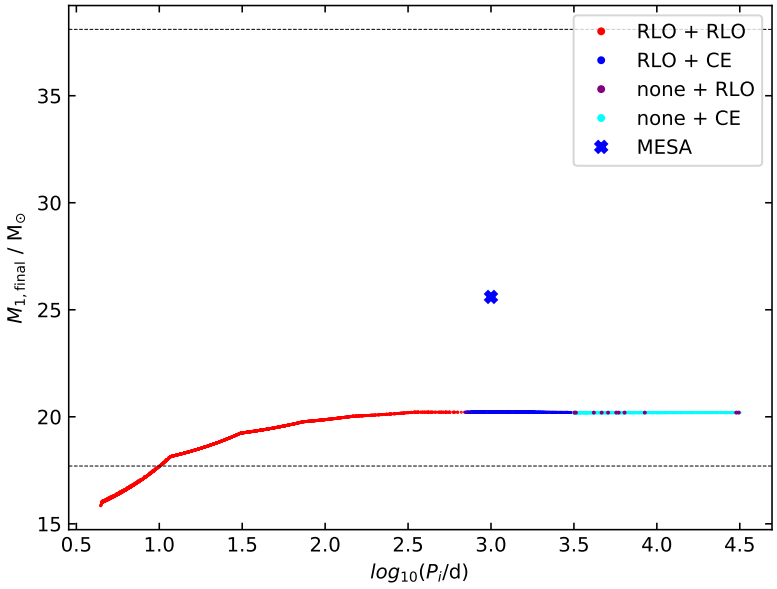

Figure 3.10: Final black hole mass of the primary component of those ComBinE systems from Fig. 3.1 with a merger time below 10^{10} yrs plotted versus their initial orbital periods. Color-coding (see legend) shows the major interactions leading to merger times within 10^{10} yrs. Additionally, the final mass of the primary component from the MESA system (see Sect. 3.3) is marked for comparison. The dashed lines represent the lower and upper limits for the primary mass of GW151012. For abbreviations, see Table 1.1.

resulting in an identical post-mass transfer mass as well, which then decreases due to wind mass loss. Therefore, the final primary mass is the same regardless of the timing of Roche-lobe overflow. If the components did not interact at all during the lifetime of the primary ($\log P_\mathrm{i} > 3.5$), the entire hydrogen envelope as well as most of the helium layer is removed in the supernova instead, which still leads to approximately the same final primary mass.

As the secondary mass depends on the entirety of the binary evolution, a lot more variation in the final value can be found in Fig. 3.11. There are differences both for systems with the same evolutionary path and between the final masses for different formation channels, although all secondaries are $\gtrsim 11\,\mathrm{M}_\odot$ and therefore definitely black holes. For the case of a stable Roche-lobe overflow from the primary before the first supernova and another from the secondary after ('RLO+RLO'), two different clusters of final masses emerge. Most systems end with a secondary mass around $\sim 13\,\mathrm{M}_\odot$. Additionally, there is a cluster of systems where the secondary has a final mass $\lesssim 12\,\mathrm{M}_\odot$, which only occurs if the system had an initial orbital period $\log P_\mathrm{i} \lesssim 1.0$.

For the 'RLO+RLO' scenario, four different combinations of stable Roche-lobe overflows are possible: case A + case A, case A + case B, case B + case A, and case B + case B. The cluster of lowest mass secondaries corresponds to case A + case A Roche-lobe overflows, where the secondary loses more mass the closer the orbital period is, analogous to the mechanism for the final primary mass. On the other hand, case A + case B mass transfers result in a final secondary mass of $\sim 13\,\mathrm{M}_\odot$. The difference is shown in the mass plots of two example systems in Fig. 3.13, a) shows case A + case A, while b) shows a system with a similar initial orbital period evolving through case A + case B Roche-lobe overflows. These different evolutionary paths at the same

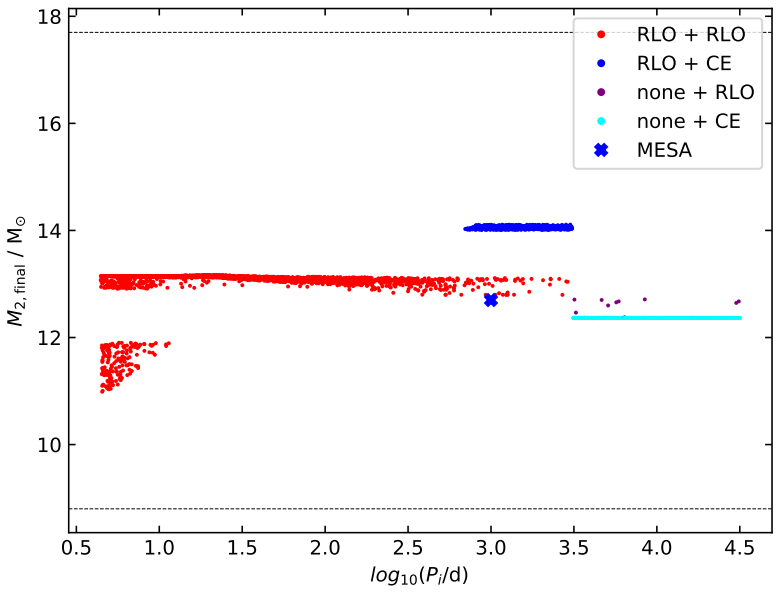

Figure 3.11: Final black hole mass of the secondary component from those ComBinE systems from Fig. 3.1 with a merger time below 10^{10} yrs plotted versus their initial orbital periods. Color-coding (see legend) shows the major interactions leading to merger times within 10^{10} yrs. Additionally, the final mass of the secondary component from the MESA system (see Sect. 3.3) is marked for comparison. The dashed lines represent the lower and upper limits for the secondary mass of GW151012. For abbreviations, see Table 1.1.

initial orbital period are introduced by the randomized impact of the supernova kick, as discussed in the previous section. This also introduces a spread in the final secondary masses because the exact timing of interaction is different for each system. This is also the case for systems with initial orbital periods large enough for the primary to undergo case B mass transfer. While the first Roche-lobe overflow leads to identical outcomes, the supernova induces different separations. Therefore, the secondary can undergo either case A or case B mass transfer, resulting in slightly different final masses.
In contrast to these mechanisms, secondaries from the standard formation channel ('RLO+CE') end up with a larger final mass of $\sim 14\,M_\odot$. An example for the mass evolution of the components in this channel is shown in Fig. 3.13 e). This is because a common envelope only sets in after hydrogen shell burning has increased the mass of the helium core (compare with Section 3.3, specifically Fig. 3.23). A convective envelope forms and prevents stable mass transfer at this point, the only possible interaction becomes common envelope evolution. Thus all systems undergoing stable Roche-lobe overflow have the same helium core mass, while all systems undergoing common envelope evolution have an increased core mass. As the fate of a common envelope is rather sensitive to the supernova kick (discussed in Section 3.2.1, Table 3.2) and subsequent post-supernova orbital period, only a small variation in the final secondary masses of this evolutionary path is introduced. The same is true if there was no interaction before the first supernova, the kick of which resulted in an orbital period where common envelope formation and ejection were possible ('none+CE', see Fig. 3.13 f)). In this case, the secondary component did not accrete any matter from the primary, resulting in a lower final mass compared to the 'RLO+CE' of $\sim 12.5\,M_\odot$.

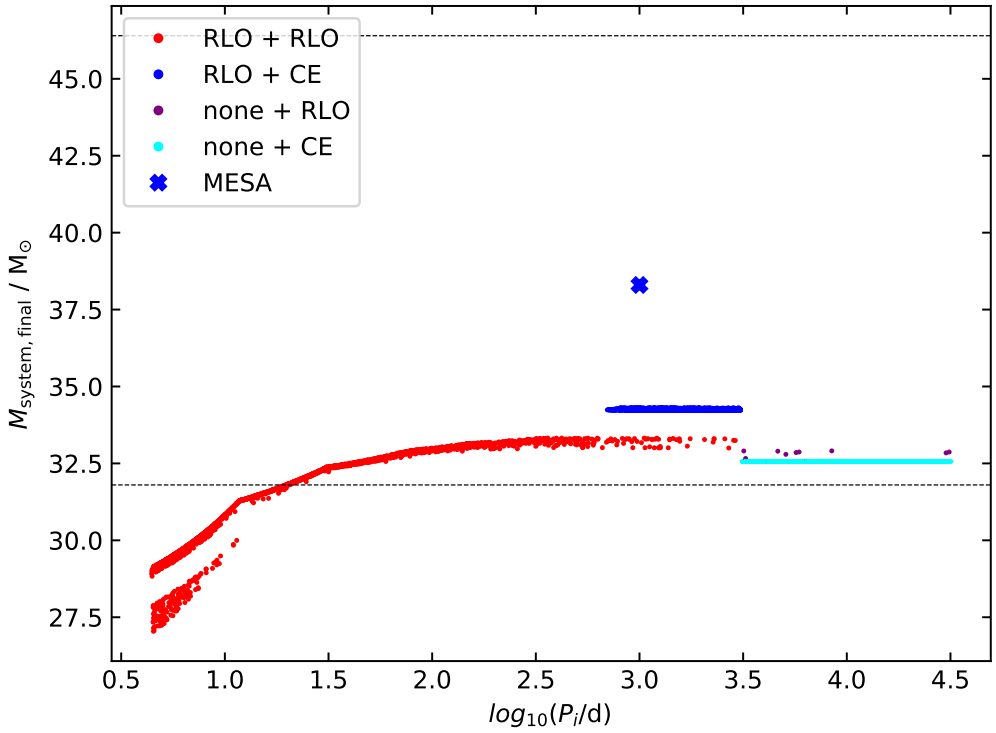

Figure 3.12: Final total mass of the ComBinE systems with a merger time below 10^{10} yrs plotted versus initial orbital period of those systems. Additionally, the final total mass of the MESA system (see Sect. 3.3) is marked for comparison. The dashed lines represent the lower and upper limits for the total mass of GW151012. For abbreviations, see Table 1.1.

The final masses for the few systems from the 'none+RLO' channel with a merger time within 10^{10} years (example in Fig. 3.13 g)) follow the same arguments, with less mass compared to the 'RLO+RLO' paths due to missing accretion from the primary. Some variation is introduced due to different timings of the Roche-lobe overflow from the secondary. Figure 3.12 shows the resulting total system masses with the lower and upper bounds given by GW151012. While even fairly close binaries could lead to a gravitational wave merger within a Hubble time according to our ComBinE models, a minimum initial orbital period of $\log P_\mathrm{i} \sim 1.3$ is needed in order to create a potential progenitor for GW151012 from systems with our initial parameters specifically. Of course this threshold would change if a variation in initial masses was introduced. Overall, the ComBinE results point to the $60 + 40\,M_\odot$ binary system at SMC metallicity being a possible progenitor at the lower end of possible masses.

The final masses of the systems, as compared to the GW151012 data, strengthen the case for the standard formation channel ('RLO+CE') further because all final masses lie firmly within the boundaries given by the event. In contrast, a significant amount of systems from the 'RLO+RLO' channel have masses that are too low to match the gravitational wave event. If we wanted to explore the formation of GW151012 progenitors undergoing case A Roche-lobe overflow specifically, we would need a larger initial primary mass. However, this would change the mass ratio of the systems, which would introduce new changes in the binary evolution.

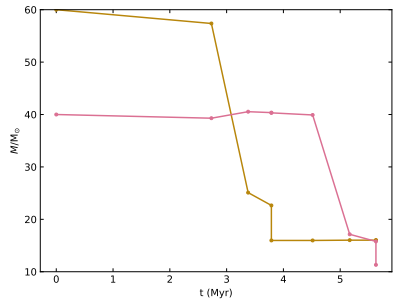

(a) RLO+RLO with P_i = 4.5 d

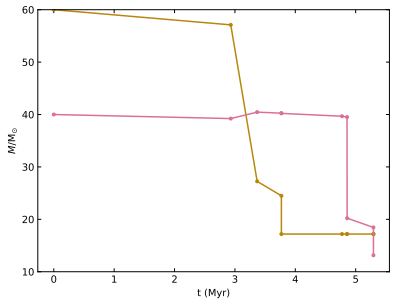

(b) RLO+RLO with P_i = 8.3 d

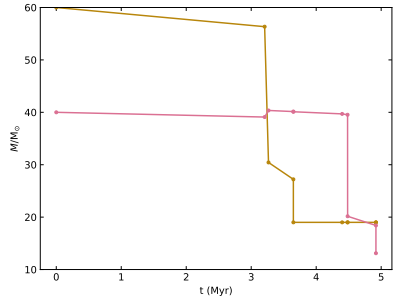

(c) RLO+RLO with P_i = 26.4 d

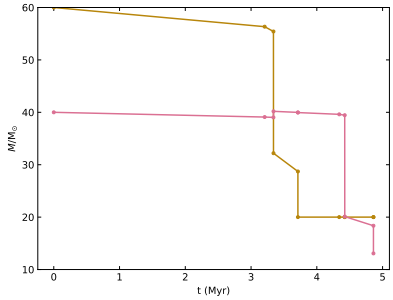

(d) RLO+RLO with P_i = 140 d

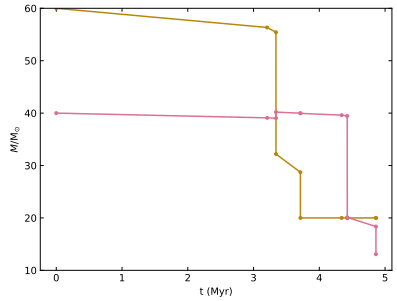

(e) RLO+CE with P_i = 3000 d

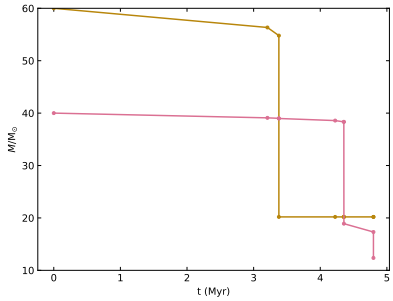

(f) none+CE with P_i = 3157 d

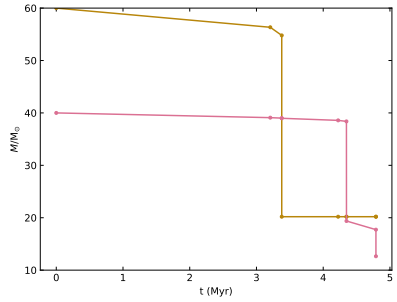

(g) none+RLO with P_i = 30216 d

(h) Legend for plots a) - g)

Figure 3.13: Plots showing the masses of both binary components versus time for selected ComBinE models from simulated systems (Fig. 3.1) with different initial orbital periods and merger times below 10^{10} yrs. Each sub caption indicates the interaction types each system goes through during its evolution and initial orbital period. Abbreviations used: RLO: Roche-lobe overflow; CE: common envelope; none: no interaction; interaction+interaction (e.g. RLO+RLO): interaction before first supernova and interaction between first and second SN.

3.2 Choosing a specific ComBinE model

In the absence of knowledge about supernova kicks (see Section 4.1.1), we follow the principle that options which need fewer assumptions are more probable. This is an indication that among the evolutionary paths present in the ComBinE models, the standard formation channel ('RLO+CE') likely contributes the most to observable gravitational wave mergers. This is already the case from the number of models merging within the Hubble time (see Fig. 3.3). Additionally, almost the entire parameter range for both supernova kicks is allowed and all binaries surviving until the binary black hole phase merge within the Hubble time.
From these results, we decided to explore a system from the 'RLO+CE' channel in detail as they point towards this evolutionary path being the most likely progenitor for GW151012 from the parameter space we studied.
First, we used ComBinE to create a more detailed system (see Section 2.1) undergoing the 'RLO+CE' evolution, which ends as a gravitational wave merger. Then we created an equivalent system in MESA (see Section 2.2), the results of both are found in the next section. The Figures 3.15 - 3.25 contain results from both ComBinE and MESA, which will first be explained separately in their respective sections before being compared.
Figure 3.14 shows termination reasons for MESA models from part of the binary grid by Chen Wang (forthcoming PhD thesis, Wang et al. (2020)) at SMC metallicity. These models are created with the same input parameters as our MESA model (see Section 2.2), which includes setting the orbital period to 10^{99} days when the primary depletes helium. Afterwards, the secondary is evolved until it depletes helium as well, provided the binary evolution is not terminated prior. While the initial primary mass ($56.2\,M_\odot$) is not identical to that of our ComBinE models ($60\,M_\odot$), we assume the binary evolution of the models to be similar enough for a comparison. The ComBinE models have an initial mass ratio of $q_i = 2/3$, which is the key column of Fig. 3.14. The reason for termination is color-coded (see legend), where most options indicate convergence errors or early mergers (e.g. "L2_overflow"). Only systems that terminate when both components have depleted helium ("Both_dep_He") have a chance to survive the entire evolution and end as a gravitational wave merger. Combining this result from Chen Wang with those from the previous section, we decided on an initial orbital period of $\log P_i = 3.0$, which equals $P_i = 1000$ days, for our detailed comparison between a ComBinE and a MESA model.

3.2.1 Detailed look at one ComBinE model

The evolutionary stages the chosen binary model underwent are presented in Table 3.1, which contains the component masses, the orbital period and eccentricity for each stage, as well as its timing. Additional information are the parameters of both supernova kicks and the parameters relevant for common envelope evolution. Figure 3.15 shows the evolution of the binary components in the Hertzsprung-Russell diagram[2]. Both components evolve as isolated stars on their respective main sequence, losing mass from stellar winds, which slightly widen the orbit.
When the more massive star ends hydrogen burning after $\sim$ 3.7 Myrs, it expands rapidly (see radius evolution in Fig. 3.17) and fills its Roche lobe, initiating mass transfer, which is marked by triangles for both components in Fig. 3.15. At this point, the secondary is still a main sequence star burning hydrogen. The mass transfer is a fast process on the thermal timescale, which causes the primary to lose more than $25\,M_\odot$, only a small amount of which ($\sim 1\,M_\odot$) can be accreted by the secondary (see mass plot in Fig. 3.19) before it reaches critical rotation.
The orbit responds to the mass transfer with widening (Fig. 3.16) due to the large amount of mass lost from the binary system. Notably, ComBinE does not include a mechanism for how the mass

[2]The HR diagram shows additional time steps for each component compared to the other plots. For the explanation, see Appendix A.1.

leaves the system, it is simply removed. The donor responds to mass loss with a shrinking radius (Fig. 3.17) because its envelope is still radiative at the onset of mass transfer, this stabilizes and then ends the mass transfer once the Roche lobe is no longer filled.
The primary is assumed to lose its entire hydrogen envelope and now follows a helium stellar track corresponding to its core mass, creating a large shift to higher temperatures in the HR diagram (see Fig. 3.15 after the first RLO). There are no further interactions before the end of its life. The position of the secondary in the HR diagram barely changes due to the low amount of accreted matter, and it continues its own evolution on the main sequence.
The supernova of the primary reduces its mass to $\sim 20\,M_\odot$ and impacts the orbital period of the system significantly. The supernova is marked with a star in Fig. 3.16 and following figures. Even though the kick velocity is moderate with $w_1 = 50\,\mathrm{km\,s^{-1}}$, the orbital period is increased to almost seven times its former value and the orbit becomes highly eccentric due to the kick angles θ_1 and φ_1 (see Table 3.1).
The supernova kick parameters were chosen deliberately to test out a 'middle of the pack' scenario of the 'RLO+CE' evolutionary path. As we have seen previously, a successful common envelope ejection can depend strongly on the parameters of the primary supernova kick. Due to our limited knowledge about kicks however, this choice is essentially no less random than any other (see Section 4.1.1). Nonetheless, it is an interesting observation that seemingly 'moderate' choices for the kick velocity can lead to such enormous changes in the orbital period.
Recircularization, which takes place over a period of time, then decreases the eccentricity back to zero, reducing the orbital period significantly, which is still almost three times as large as the pre-supernova value. About 4.5 Myrs after the zero-age main sequence, the secondary has itself become a helium burning star and expands, filling its Roche lobe (again marked with a triangle in Fig. 3.15). This time however, due to the larger binary separation (Fig. 3.16) and lower mass of the secondary (Fig. 3.19) compared to the first mass transfer, the secondary has to reach a larger radius (Fig. 3.17) until it fills its Roche lobe. At this point, the envelope has become sufficiently convective to destabilize the mass transfer and common envelope evolution starts.
Whether the envelope can be ejected depends on its binding energy, which is shown in Figure 3.18 as calculated according to Eq. 1.5 (see Section 2.1.3). Once the envelope becomes convective, it becomes far less strongly bound, enabling its ejection. We can see that even a slightly smaller value for the orbital separation, equivalent to an earlier onset of the common envelope evolution, due to a different supernova kick could prevent a successful envelope ejection and lead to a merger of the binary instead.
This hypothesis was tested with several ComBinE systems that had identical parameters to our chosen one, except for different velocities in the first supernova kick, the result of which is presented in Table 3.2. The outcome of the common envelope for this specific system in ComBinE is indeed very sensitive to the kick velocity, predicting envelope ejection only for kick velocities $40 < w_1 < 55\,\mathrm{km\,s^{-1}}$. The exact values will be different depending on the binary system's initial parameters as well as the values for the kick angles θ_1 and φ_1. Assuming different ejection efficiency parameters for the common envelope evolution (Section 4.1.1) would also change the results. The crucial conclusion to this observation is the strong dependence on the presence and strength of the first supernova kick for the outcome of a given binary system.
For our chosen values of $w_1 = 50\,\mathrm{km\,s^{-1}}$ and $\alpha_{\mathrm{CE}} = 0.5$, the envelope is successfully ejected, leaving the secondary as a naked helium star of $\sim 21\,M_\odot$ in an extremely tight binary with the primary black hole (see Fig. 3.16). The components do not interact anymore as the secondary only shrinks in its further evolution (Figs. 3.17 and 3.24). Wind mass loss decreases the secondary's mass to $\sim 20\,M_\odot$ prior to its supernova (Fig. 3.19), which widens the orbit but not to a significant degree (see Figs. 3.16 and 3.25).

Even though the secondary supernova kick velocity was chosen to be twice the value of w_1, with randomly chosen values for the kick angles θ_2 and φ_2, it cannot significantly affect the orbital period anymore. This agrees with our results from Section 3.1.1 that the second supernova is irrelevant to the outcome for this evolutionary path.
The binary evolution ends with two black holes with $M_1 = 20.2\,M_\odot$ and $M_2 = 14.1\,M_\odot$ and an orbital period of $P_{\mathrm{orb,\,final}} = 0.238$ days. 10.6 Myrs after the zero-age main sequence, the black holes finally merge in a gravitational wave event, the timing of which is right in the middle of the range of merger times for the 'RLO+CE' channel systems we studied ($10^6 - 10^8$ years, see Fig. 3.2). Overall, the system closely follows the evolutionary stages of the established standard channel for binary black hole formation (Belczynski et al. (2016)).

3.3 Detailed model of a binary with MESA

The binary system investigated with MESA undergoes many of the same evolutionary stages as the ComBinE model, which are also presented in Table 3.1. Kippenhahn diagrams allow us to show interior changes to a star, which are presented in Figs. 3.20 and 3.21 for the primary, as well as Figs. 3.22 and 3.23 for the secondary, showing the types of mixing occurring within the stars as well as helium abundance and the nuclear burning generation rate ϵ_{nuc} in gray-scale. As long as the primary burns hydrogen in its core (ϵ_{nuc} is shown in gray-scale in Fig. 3.21), the stars remain isolated and evolve along their respective main sequences (see HR diagram in Fig. 3.15).
Once hydrogen is depleted after ~ 4 Myrs, mass transfer is initiated from the primary to the secondary (marked with triangles in Fig. 3.15), caused by the primary's rapid envelope expansion (Fig. 3.17). The mass transfer occurs quickly on the thermal timescale of the star, removing almost $\sim 20\,M_\odot$ of the primary's envelope. Part of the primary's envelope has already become convective at this point, but not by such an amount that it would destabilize the mass transfer.
The mass transfer removes most of, but not the entire envelope. Crucially, the hydrogen burning layer remains (see Fig. 3.21, which increases the mass of the helium core over time. The secondary can only accrete a small amount of the primary's lost mass ($\sim 0.3\,M_\odot$) before it approaches critical rotation, preventing further accretion in the model (see Section 2.2). The remainder of the mass is assumed to leave the system.
As the mass transfer reaches helium-enriched layers of the primary (see gray-scale in Fig. 3.20), the accreted mass contains more helium than the surface of the secondary, triggering thermohaline mixing (Fig. 3.22). The primary responds to the mass loss with shrinking, while the secondary expands slightly from the mass gain (Fig. 3.17). The primary's shrinking allows the binary to detach after a short time, resulting in the components evolving independently again. The primary continues its evolution as an almost naked helium star, while the secondary follows almost the same main sequence as before (Fig. 3.15) because the accreted matter represents less than 1% of its total mass. The orbital period of the system is also affected by the mass transfer (Fig. 3.16) because the mass lost from the system slightly widens it, increasing the orbital period to about 1.06 times its former value (see Table 3.1).
In its further evolution during helium burning, the primary expands again (Fig. 3.17), but far less strongly than before, which is not enough to trigger another Roche-lobe overflow. The MESA model of the primary is stopped when it is helium depleted (see Section 2.2 for specifics). In MESA, the orbital period is set to 10^{99} days, but in our complete model, we calculated the post-supernova orbital period according to Eq. 2.5, using the same values for the kick parameters we used in the previously discussed ComBinE model. The orbital period increases to more than four times its pre-supernova value. Our approximation for recircularization is applied immediately, after which the orbital period is kept constant until the next interaction. This effect creates the peak visible in Fig. 3.16.

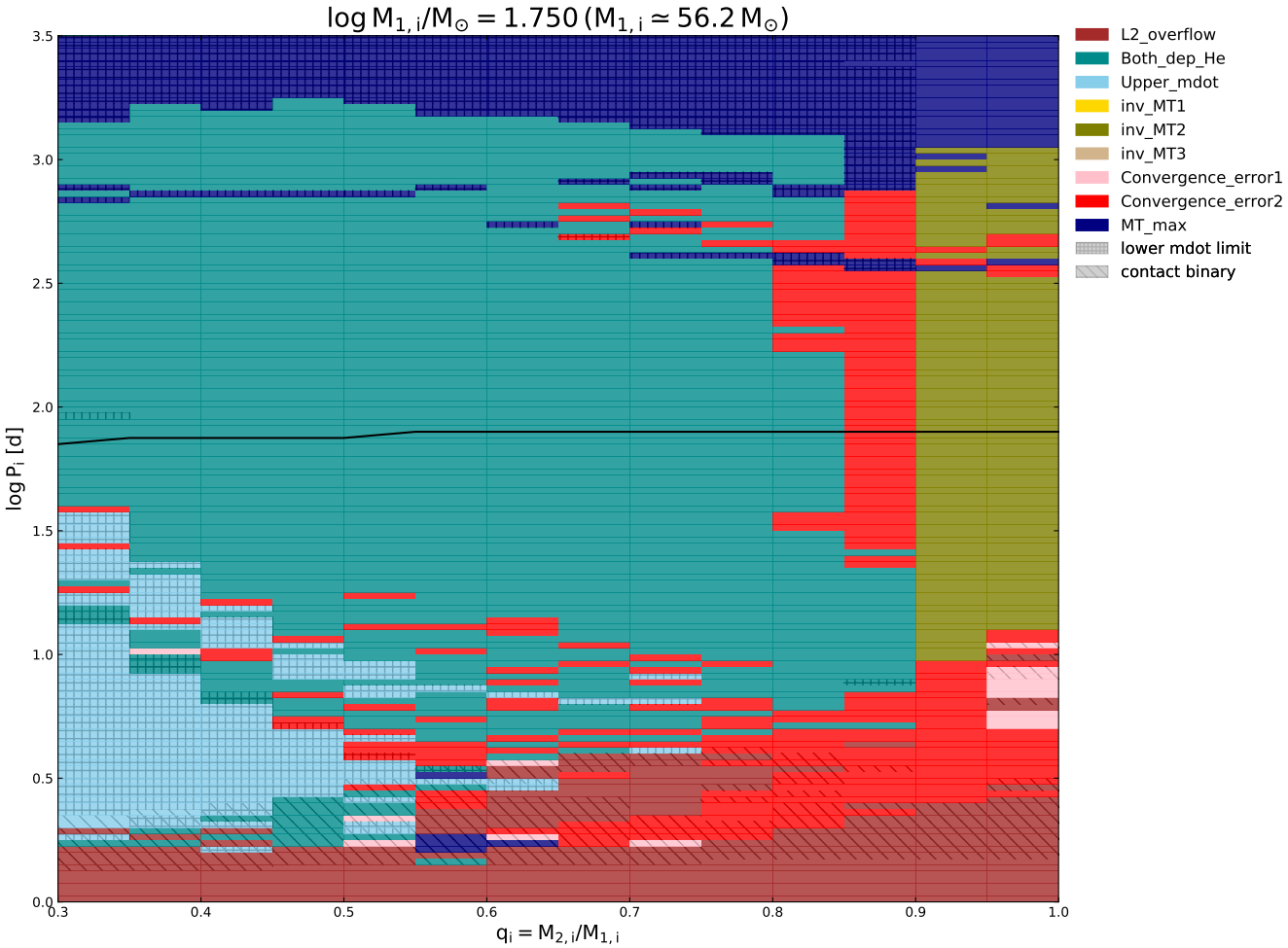

Figure 3.14: Plot showing termination reasons (color-coded, see legend) for a grid of binary MESA models with different initial orbital periods and mass ratios for a primary mass of $\sim 56.2\,M_\odot$ at SMC metallicity. Taken from PhD thesis of Chen Wang (to be released). "Both_dep_He" means that both model components can deplete helium, with the orbital period set to infinity after the primary has depleted helium (same treatment as in my model, see Section 2.2). All other termination reasons prevent the model from reaching the binary black hole phase.

Table 3.1: Table showing the significant evolutionary stages of the ComBinE model described in Section 3.1 compared with their equivalents in the MESA model described in Section 3.3. For each stage, significant parameters of both models are shown. Abbreviations used: ZAMS: zero-age main sequence; RLO: Roche-lobe overflow; SN: supernova; CE: common envelope; BH: black hole; GW: gravitational wave event.

Events	ComBinE	MESA
ZAMS	$M_1 = 60.0\,\mathrm{M}_\odot$ $M_2 = 40.0\,\mathrm{M}_\odot$ $\mathrm{P}_{\mathrm{orb}} = 1000$ days, $e = 0$ $a = 1955\,\mathrm{R}_\odot$	$M_1 = 60.0\,\mathrm{M}_\odot$ $M_2 = 40.0\,\mathrm{M}_\odot$ $\mathrm{P}_{\mathrm{orb}} = 1000$ days, $e = 0$
RLO primary to secondary $t = 3.37$ Myr (ComBinE) $t = 4.01$ Myr (MESA)	$M_1 = 54.9\,\mathrm{M}_\odot$ (He-burning star) $M_2 = 39.0\,\mathrm{M}_\odot$ $\mathrm{P}_{\mathrm{orb}} = 1138$ days	$M_1 = 55.3\,\mathrm{M}_\odot$ (He-burning star) $M_2 = 38.9\,\mathrm{M}_\odot$ $\mathrm{P}_{\mathrm{orb}} = 1123$ days
SN of primary $t = 3.74$ Myr (ComBinE) $t = 4.32$ Myr (MESA) $w = 50\,\mathrm{km\,s^{-1}}$ $\theta = 90°$ $\varphi = 90°$	$M_1 = 29.0\,\mathrm{M}_\odot$ $M_1 = 39.9\,\mathrm{M}_\odot$ $\mathrm{P}_{\mathrm{orb}} = 1853$ days after SN: $M_1 = 20.2\,\mathrm{M}_\odot$ (BH) $M_2 = 39.9\,\mathrm{M}_\odot$ (H-burning star) $\mathrm{P}_{\mathrm{orb}} = 12967$ days $e = 0.714$	$M_1 = 35.7\,\mathrm{M}_\odot$ $M_2 = 39.2\,\mathrm{M}_\odot$ $\mathrm{P}_{\mathrm{orb}} = 1382$ days after SN: $M_1 = 25.6\,\mathrm{M}_\odot$ (BH) $M_2 = 39.2\,\mathrm{M}_\odot$ (H-burning star, mass assumed unchanged) $\mathrm{P}_{\mathrm{orb}} = 5498$ days $e = 0.790$
RLO secondary to primary results in CE $t = 4.53$ Myr (ComBinE) $t = 5.19$ Myr (MESA)	$M_1 = 20.2\,\mathrm{M}_\odot$ $M_2 = 36.0\,\mathrm{M}_\odot$ (He-burning star) $\mathrm{P}_{\mathrm{orb}} = 5091$ days $e = 0$ $\lambda = 0.0076$, $\alpha_{\mathrm{CE}} = 0.5$	$M_1 = 25.6\,\mathrm{M}_\odot$ $M_2 = 38.2\,\mathrm{M}_\odot$ (He-burning star) $\mathrm{P}_{\mathrm{orb}} = 1087$ days $e = 0$ $E_{\mathrm{bind}} = -1.2 \times 10^{50}$ erg, $\alpha_{\mathrm{CE}} = 0.5$
CE ejection $t = 4.53$ Myr (ComBinE) $t = 5.19$ Myr (MESA)	$M_1 = 20.2\,\mathrm{M}_\odot$ $M_2 = 20.6\,\mathrm{M}_\odot$ (naked He star) $\mathrm{P}_{\mathrm{orb}} = 0.185$ days	$M_1 = 25.6\,\mathrm{M}_\odot$ (BH, mass assumed unchanged) $M_2 = 19.1\,\mathrm{M}_\odot$ (approximate with He ZAMS star) $\mathrm{P}_{\mathrm{orb}} = 0.128$ days
RLO secondary to primary $t = 5.20$ Myr (MESA)	no RLO	$M_1 = 25.6\,\mathrm{M}_\odot$ $M_2 = 18.5\,\mathrm{M}_\odot$ (He-burning star) $\mathrm{P}_{\mathrm{orb}} = 0.128$ days
SN of secondary $t = 4.76$ Myr (ComBinE) $t = 5.58$ Myr (MESA) $w = 100\,\mathrm{km\,s^{-1}}$ $\theta = 119°$ $\varphi = 285°$	$M_1 = 20.2\,\mathrm{M}_\odot$ $M_2 = 19.8\,\mathrm{M}_\odot$ $\mathrm{P}_{\mathrm{orb}} = 0.192$ days after SN: $M_1 = 20.2\,\mathrm{M}_\odot$ $M_2 = 14.1\,\mathrm{M}_\odot$ $\mathrm{P}_{\mathrm{orb}} = 0.238$ days $e = 0.089$	$M_1 = 25.7\,\mathrm{M}_\odot$ $M_2 = 16.5\,\mathrm{M}_\odot$ $\mathrm{P}_{\mathrm{orb}} = 0.131$ days after SN: $M_1 = 25.7\,\mathrm{M}_\odot$ $M_2 = 12.7\,\mathrm{M}_\odot$ $\mathrm{P}_{\mathrm{orb}} = 0.138$ days $e = 0.266$
GW merger $t = 16$ Myr (ComBinE) $t = 7.7$ Myr (MESA)	$M_{\mathrm{system}} = 34.3\,\mathrm{M}_\odot$ $q = 0.7$	$M_{\mathrm{system}} = 38.4\,\mathrm{M}_\odot$ $q = 0.5$

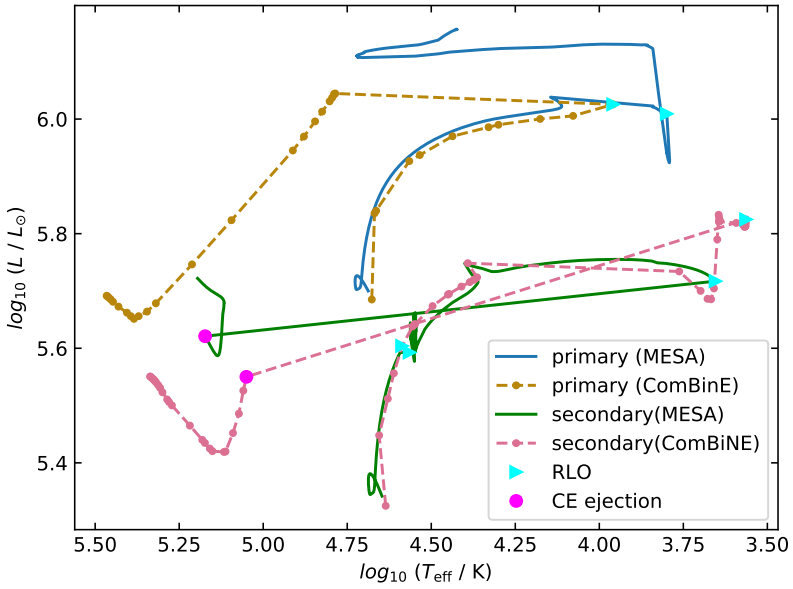

Figure 3.15: Hertzsprung-Russel diagram of the stars in the binary system with $M_1 = 60\,\mathrm{M}_\odot$ (higher luminosity), $M_2 = 40\,\mathrm{M}_\odot$ (lower luminosity) and an initial orbital period of 1000 days at SMC metallicity, without initial eccentricity. Shown is a comparison between the evolutionary tracks of the ComBinE (dashed) and the MESA models, see Sections 3.1 and 3.3 respectively. The triangles indicate the onset of Roche-lobe overflows, the second of which results in a common envelope. The CE ejection is marked by circles in both the ComBinE and MESA secondary. For both ComBinE and MESA, the model with onset of the second RLO is followed by the model of CE ejection, the CE itself is not modelled. For abbreviations, see Table 1.1.

Due to our assumptions, the secondary is not impacted by the supernova of the primary. It is instead allowed to continue evolving along its main sequence until the core depletes hydrogen. The MESA model then continues its evolution until helium depletion (see Fig. 3.22).

After leaving its main sequence at ~ 5.2 Myrs, the envelope of the secondary becomes convective as the core contracts in order to ignite helium. Outside the core, hydrogen layer burning begins, as can be seen in Fig. 3.23, which increases the helium core mass over time. At the same time, the envelope begins rapid expansion (Fig. 3.17), which causes it to fill its Roche lobe. The timing of this depends on the orbital period of the binary components. This event is marked by a second triangle in the HR diagram (Fig. 3.15) and a yellow line in the Kippenhahn diagram (Fig. 3.22). As shown in the Kippenhahn diagrams, a significant part of the envelope is convective at this point, destabilizing the mass transfer and triggering the common envelope evolution. Our code does not provide spatial or time resolution for the common envelope evolution, only its outcome is calculated. With the assumptions made in Section 2.2, including an ejection efficiency parameter of $\alpha_{\rm CE} = 0.5$, the system can eject the envelope, resulting in an orbital period of $P_{\rm orb} = 0.128$ days. Fig. 3.18 shows the binding energy of the envelope, which demonstrates how much less tightly the envelope becomes bound when the secondary expands, right at the onset of common envelope.

The successful envelope ejection hinges on the orbital period at the onset of common envelope, which in turn depends on the supernova kick. This dependence is investigated and presented in Table 3.2, which shows that the window for the kick velocity in this specific model ranges from

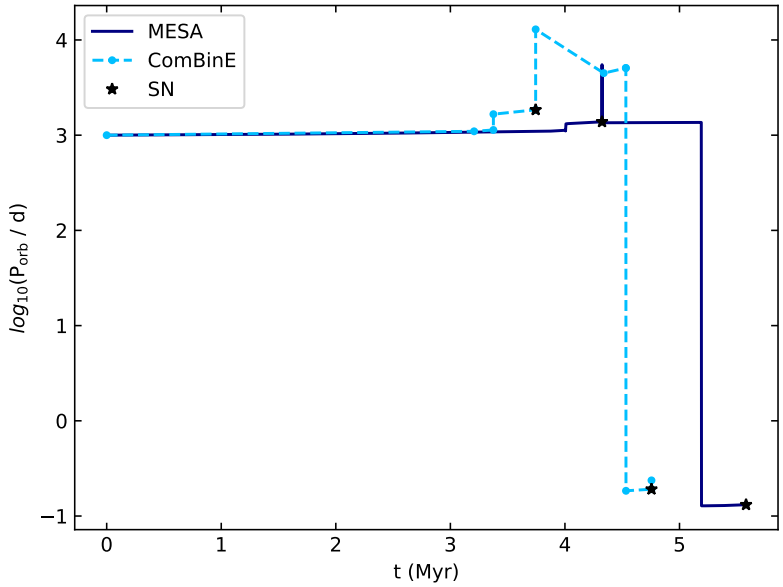

Figure 3.16: Orbital period evolution of the binary system in the ComBinE and the MESA models from Fig. 3.15 over time. The dashed line shows the orbital period for the ComBinE model. The supernovae of the primary and the secondary star are marked with star symbols. For the MESA model, orbital period between the first SN and CE ejection is not modelled and instead assumed constant (see Sec. 2.2). For abbreviations, see Table 1.1.

$\sim 25\,\mathrm{km\,s^{-1}}$ to $\sim 55\,\mathrm{km\,s^{-1}}$, assuming identical values for the kick angles. For our model, we can also calculate the needed value for the ejection efficiency parameter that results in the minimum orbital separation after envelope ejection. The minimum separation is defined to be the point where the Roche-lobe radius of the secondary's core equals its radius ($R_{2,\mathrm{RL}} = R_{2,\mathrm{core}}$, see Eq. 2.11). This still allows the binary to detach after envelope ejection, which now consists of the secondary's core and a black hole. The calculated values for α_{CE} at different kick velocities are also presented in Table 3.2. The larger the kick, and therefore the post-supernova binary separation, the later the common envelope sets in and the envelope becomes less tightly bound. This allows an envelope ejection even for lower ejection efficiencies, which is explored further in Section 3.3.2.
The smallest kick velocity with a possible envelope ejection for this model is $w_1 \sim 25\,\mathrm{km\,s^{-1}}$, resulting in a slightly earlier onset than with our standard value of $w_1 = 50\,\mathrm{km\,s^{-1}}$. At this earliest point, a sufficient fraction of the envelope is convective (14% of the stellar mass, see Section 2.2) to trigger the common envelope event in the first place, therefore this is also the case for larger kick velocities resulting in later onsets of mass transfer.
Table 3.1 showing the evolutionary stages of the binary contains the values for the components after envelope ejection resulting from a supernova kick velocity of $w_1 = 50\,\mathrm{km\,s^{-1}}$, with an envelope ejection efficiency parameter of $\alpha_{\mathrm{CE}} = 0.5$ to maintain comparability with the ComBinE system.

3.3.1 Second MESA binary model for the components after common envelope evolution

After the common envelope is ejected, the binary evolution module for MESA is used to set up a new run (see Section 2.2.4) with a $25.6\,\mathrm{M_\odot}$ point mass and a $19.1\,\mathrm{M_\odot}$ zero-age helium main

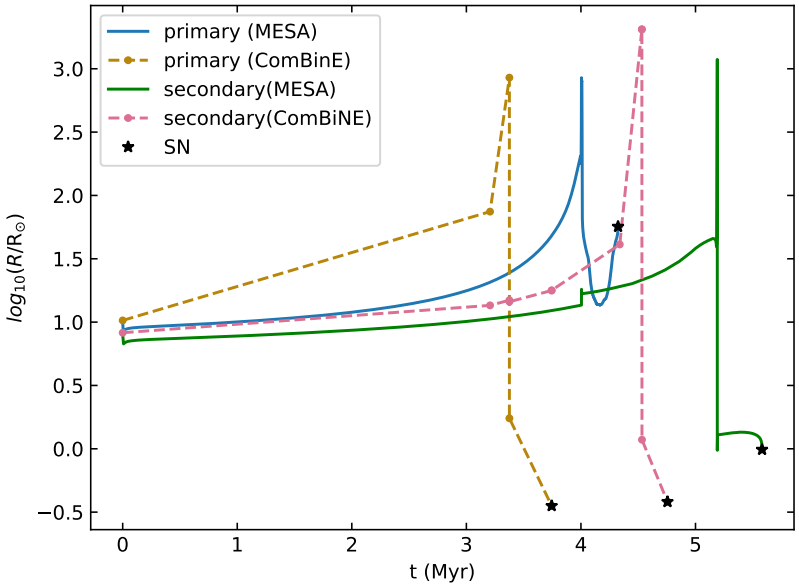

Figure 3.17: Radius evolution of both stellar components for the ComBinE and MESA from Fig. 3.15. Dashed lines are for the components of the ComBinE model, solid for MESA. The supernova of each component is marked by a star symbol.

sequence star at an initial orbital period of $P_{\mathrm{orb}} = 0.128$ days. The evolution of the secondary in the HR diagram after common envelope is shown in Fig. 3.15 as well, with the envelope ejection point marked in magenta. The radius evolution of the helium star as well as its Roche-lobe radius is shown in Fig. 3.24. The strong increase in radius at the start of modelling (from $\sim 1.0\,\mathrm{R}_\odot$ to $\sim 1.3\,\mathrm{R}_\odot$) is an artifact of modelling and can be disregarded. During helium burning, the secondary slightly expands, which due to the closeness of the components is enough to fill its Roche lobe again ~ 0.1 Myr after the common envelope.
The mass transfer causes the secondary to lose $\sim 2\,\mathrm{M}_\odot$ of its mass, $\sim 0.1\,\mathrm{M}_\odot$ of which is accreted by the black hole, the remainder is lost. While the Roche lobe is filled (until ~ 0.33 Myr after common envelope), the orbital period of the system slightly increases due to the mass loss (Fig. 3.25). Once helium is depleted, the evolution of the secondary is stopped and the supernova treatment (see Section 2.2) is applied with the same parameters used in the ComBinE model (see Table 3.1), which results in an orbital period of $P_{\mathrm{orb}} = 0.138$ days and an eccentricity of $e = 0.266$ for the system, now consisting of two black holes. Their final masses are $25.7\,\mathrm{M}_\odot$ for the primary and $12.7\,\mathrm{M}_\odot$ for the secondary. As the secondary was already stripped of its entire envelope, it lost $< 4\,\mathrm{M}_\odot$ of its mass in the supernova.
Around 7.7 Myrs after the zero-age main sequence of both stellar models, the black holes finally merge in a gravitational wave event, with a total system mass of $M = 38.4\,\mathrm{M}_\odot$.

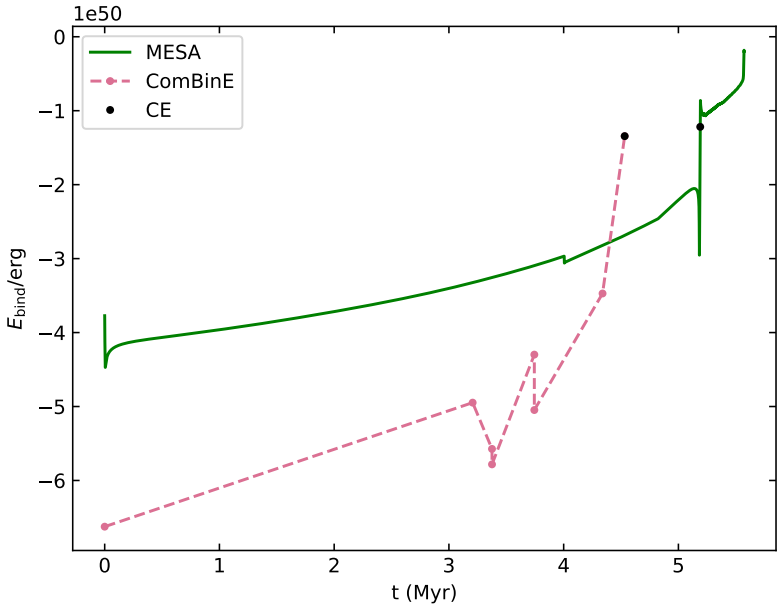

Figure 3.18: Evolution of the envelope binding energy in the secondary star over time with a comparison between the ComBinE (dashed line) and MESA (solid) model. Onset of common envelope is indicated with a circle for each model. As the envelope is ejected after CE, calculation of binding energy stops after this point in the ComBinE model. In the MESA model, the secondary is evolved as a single star until helium depletion, allowing the calculation of the envelope binding energy until that point. For abbreviations, see Table 1.1.

Table 3.2: Outcome of using different kick velocities in the first supernova with otherwise identical parameters, including kick angles. A specific ComBinE system as described in Section 3.1 with its equivalent MESA system, described in Section 3.3 , are compared.

w_1 / km s^{-1}	ComBinE outcome	post-CE P_{orb}/ d (ComBinE)	MESA outcome $\alpha_{\mathrm{CE}} = 0.5$	post-CE P_{orb}/ d, $\alpha_{\mathrm{CE}} = 0.5$ (MESA)	α_{CE} for $P_{\mathrm{orb,min}}$ (MESA)
0	CE merger	N/A	CE merger (Note: See Appendix A.1)	N/A	N/A
10	CE merger	N/A	stable RLO	N/A	N/A
20	CE merger	N/A	CE merger	N/A	0.56
25	CE merger	N/A	CE ejection	0.062	0.50
30	CE merger	N/A	CE ejection	0.072	0.44
40	CE merger	N/A	CE ejection	0.091	0.36
45	CE ejection	0.135	CE ejection	0.105	0.33
50	CE ejection	0.185	CE ejection	0.128	0.31
55	No interactions after 1st SN	N/A	CE ejection	0.147	0.26
60	No interactions after 1st SN	N/A	No interactions after 1st SN	N/A	N/A
70	system destroyed by 1st SN	N/A	system destroyed by 1st SN	N/A	N/A

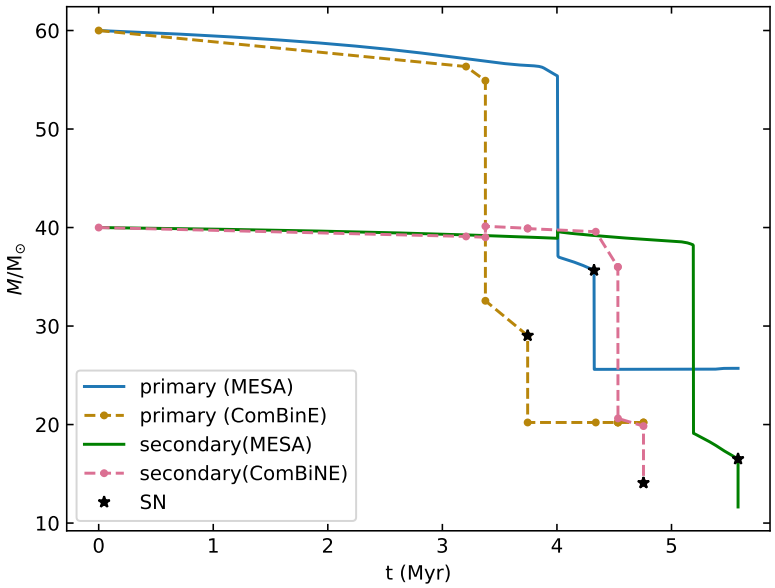

Figure 3.19: Plot showing the masses of both component stars as modelled in ComBinE (dashed lines) and MESA (solid) versus time. The primary mass starts at $60.0\,M_\odot$, the secondary mass at $40.0\,M_\odot$. For each component, the supernova is indicated by a star symbol, after which the black hole mass is shown, as calculated following the description in Chapter 2.

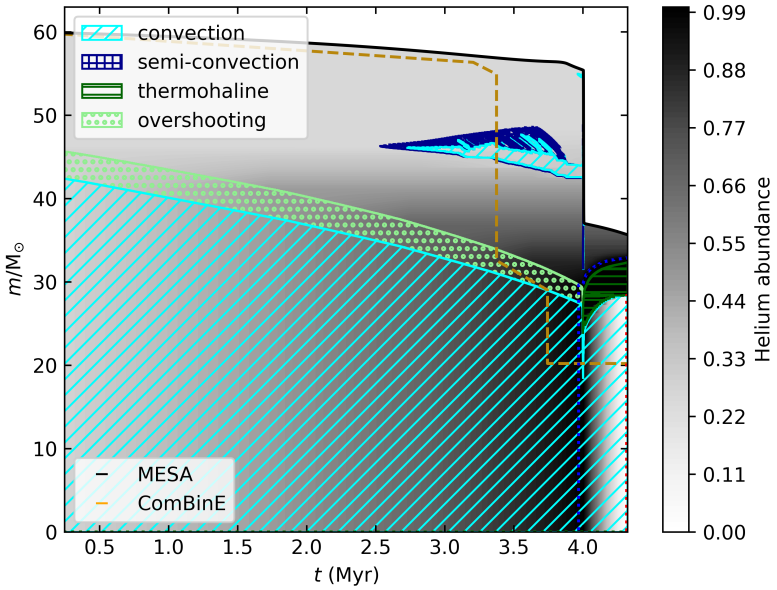

Figure 3.20: Kippenhahn diagram of the primary component in the MESA model from zero-age main sequence (ZAMS) to helium depletion. The gray-scale shows He abundance in the star and mixing type is indicated with hatching types (see legend). The mass evolution over time for the primary star from the ComBinE model is overlaid as a dashed line.

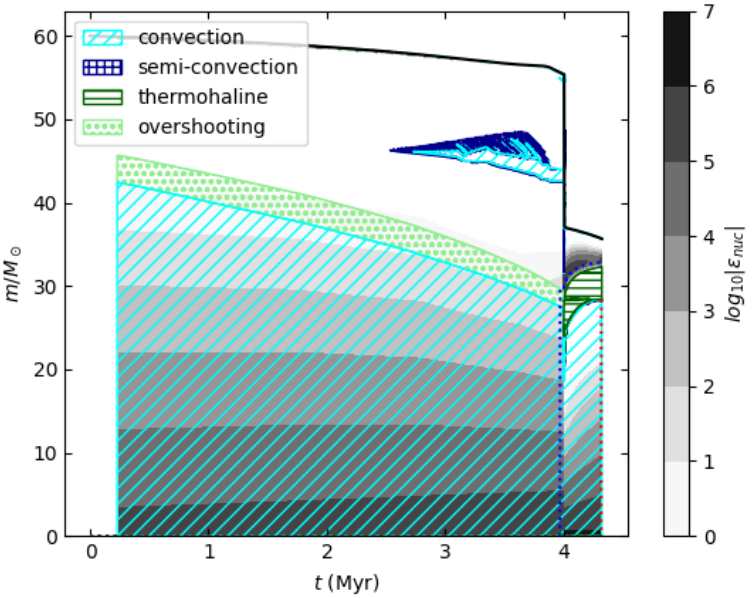

Figure 3.21: Kippenhahn diagram for the primary star from the same MESA model as before (Fig. 3.20), showing the nuclear burning generation rate ϵ_{nuc} throughout the star in gray-scale. The hatching types show mixing type (see legend), identical to Fig. 3.20.

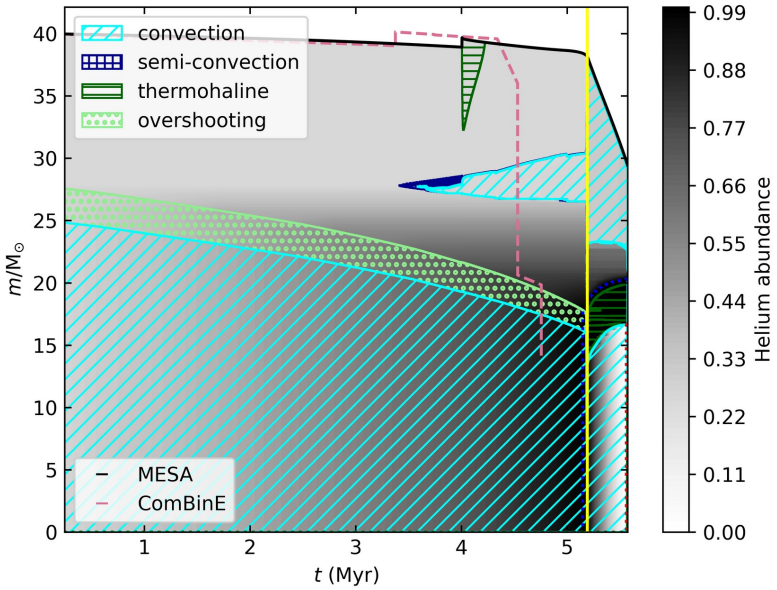

Figure 3.22: Kippenhahn diagram of the secondary component in the MESA model from ZAMS to helium depletion. The gray-scale shows He abundance in the star and mixing type is indicated with hatching types (see legend). The mass evolution over time for the secondary star from the ComBinE model is overlaid as a dashed line. Onset of common envelope evolution in the MESA model is indicated by the yellow line.

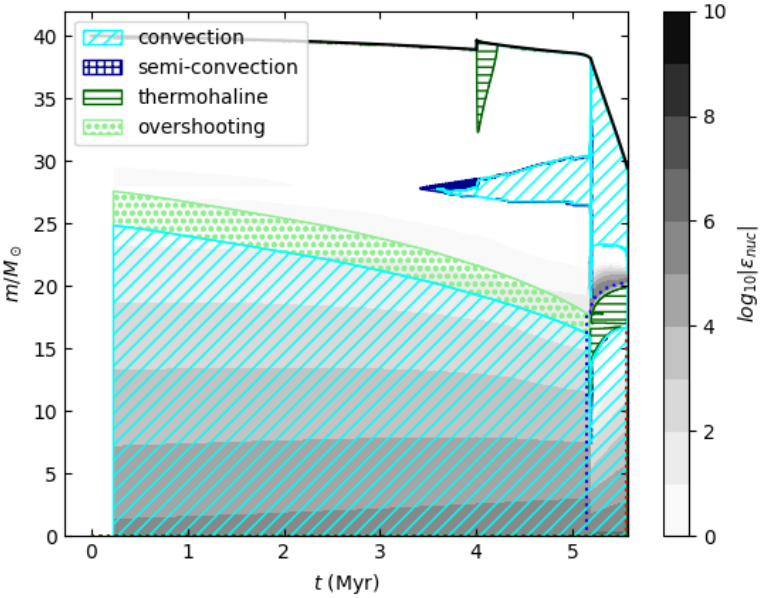

Figure 3.23: Kippenhahn diagram for the secondary star from the same MESA model as before (Fig. 3.22), showing the nuclear burning generation rate ϵ_{nuc} throughout the star in gray-scale. The hatching types show mixing type (see legend), same as Fig. 3.22.

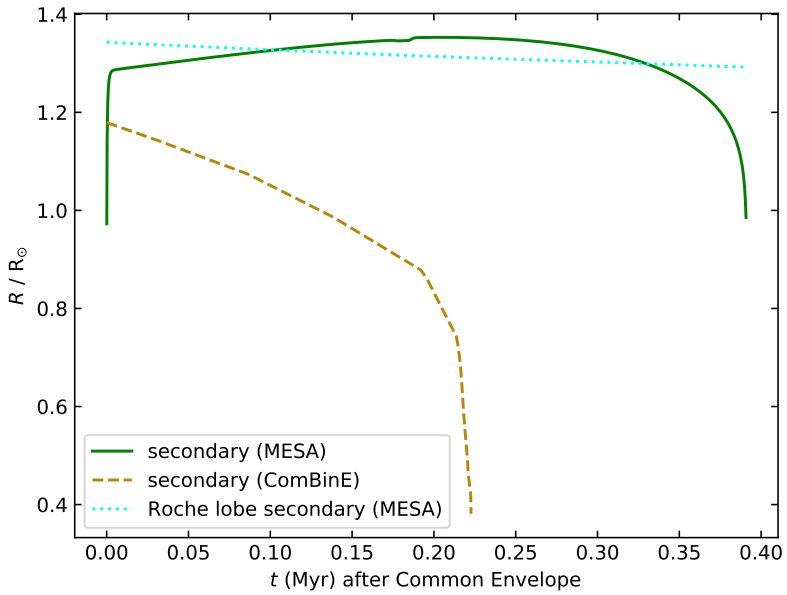

Figure 3.24: Comparing radius evolution of the secondary component in the MESA and ComBinE models after the common envelope has been ejected. Additionally, the Roche lobe radius of the secondary as calculated with MESA is shown.

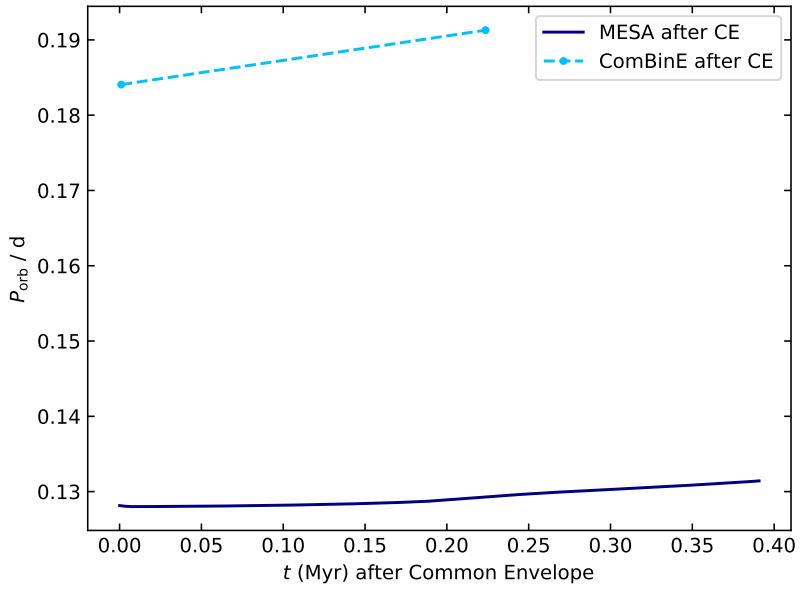

Figure 3.25: Comparing evolution of the orbital period after common envelope ejection in the MESA and ComBinE models.

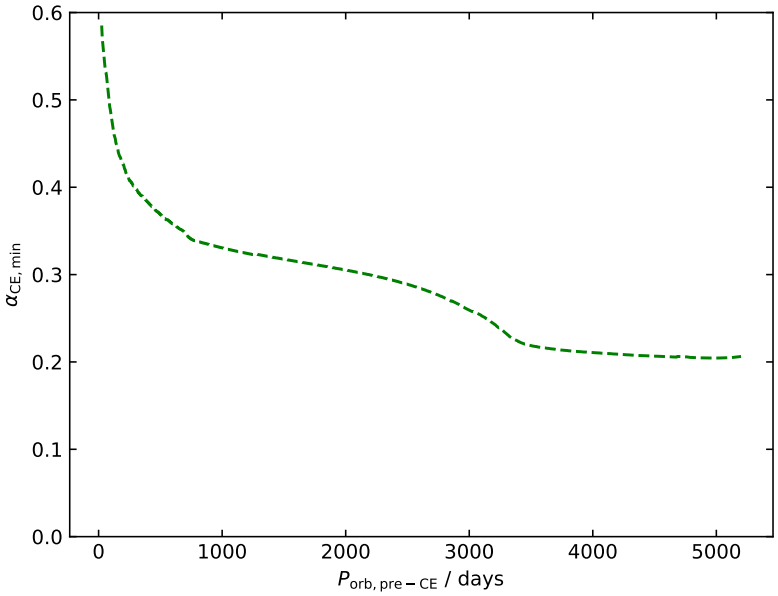

Figure 3.26: Minimum ejection efficiency parameter α_{CE} needed for the successful common envelope (CE) evolution for different pre-CE orbital periods assuming recircularization prior to mass transfer. The plot is based on the MESA binary model with initial conditions as in Section 2.2. Instead of using the developed code to determine pre-CE orbital period from a specific supernova kick, a value for this parameter is assumed (presented on the x-axis) and the outcome calculated following the same prescription as in Section 2.2.3.

3.3.2 Outcome of the common envelope evolution for different orbital periods

We adapted our code to systematically calculate the needed ejection efficiency parameter for different orbital periods of the model at the onset of common envelope evolution. For this, the supernova calculation regarding ejected mass was still used, and only the post-supernova orbital period after recircularization was replaced. From Equation 2.11, we can see that the ejection efficiency for the minimum binary separation, which is proportional to $P_{\mathrm{orb,\,min}}$, is also the minimum value the common envelope evolution needs in order for the envelope to be ejected at all. The results are presented in Figure 3.26, starting at the smallest orbital period where common envelope evolution is predicted to occur instead of a stable Roche-lobe overflow ($P_{\mathrm{orb}} \sim 25$ days). $\alpha_{\mathrm{CE,\,min}}$ is calculated up to an pre-common envelope orbital period of 5200 days. For binaries significantly wider than this, the code predicts the components to not interact at all.

A larger orbital period prior to common envelope is equivalent to a later onset of common envelope evolution, although the scaling is not the same, because the expansion of the secondary component at this point is extremely fast. With increasing age of the secondary model, its core mass increases slightly due to hydrogen layer burning (see Fig. 3.23). At the same time, its core radius decreases, as the core contracts until it is hot enough too ignite helium. As a result, the minimum orbital period (Eq. 2.12) is decreased for later onset of common envelope. The difference is slight however, from ~ 0.062 days for the earliest successful common envelope, down to ~ 0.055 days for the late interactions (calculated for $w_1 = 25\,\mathrm{km\,s^{-1}}$ and $w_1 = 55\,\mathrm{km\,s^{-1}}$ respectively).

The needed ejection efficiency decreases with increasing pre-common envelope orbital period.

The decrease doesn't have the same slope throughout. Instead, it follows a similar pattern to the envelope binding energy, shown in Fig. 3.18, which the ejection efficiency parameter is directly proportional to. Differently to the binding energy however, $\alpha_{\mathrm{CE,\,min}}$ doesn't have regions where its value increases with increasing orbital period[3]. This is because $|\Delta E_{\mathrm{orb}}|$, the other side of the energy budget, increases with increasing pre-common envelope orbital period as well, as more energy can be released by the in-spiral until the minimum orbital period is reached.
Only for the smallest orbital periods an ejection efficiency larger than $\alpha_{\mathrm{CE}} = 0.5$ is needed, which is the value assumed in ComBinE. Therefore, if $\alpha_{\mathrm{CE}} = 0.5$ is a realistic value, MESA predicts that all but the initially closest common envelope evolutions can end successfully without the components merging. We also saw this result in Table 3.2, where the model with a kick velocity of $w_1 = 25\,\mathrm{km\,s^{-1}}$ is already able to eject the envelope, with its post-common envelope orbital period also representing the minimum orbital period. Any lower kick velocities would result in closer binary components, which would require a ejection efficiency $\gtrsim 0.5$ to eject the common envelope. Whether the value is realistic will be discussed in Section 4.1.1.
In principle, we don't know whether a successful common envelope evolution that ends at or close to the minimum orbital period would survive the rest of the binary evolution. Our MESA model experiences and survives another Roche-lobe overflow after common envelope evolution, which would suggest that this would also be possible for models that end up with a smaller separation. However, the minimum orbital period is extremely small. Being this close together could conceivably trigger instabilities in the mass transfer that are not existent for the model we evolved.

3.4 Comparison ComBinE and MESA results

The ComBinE model from Section 3.2.1 and the MESA model from Section 3.3 are fairly similar overall, with significant differences in the course of their evolutionary stages, which we will discuss in this section.
Firstly, the timing stands out, as the ComBinE model evolves faster than the MESA model. This is a general difference between the two evolutionary codes[4], which can therefore be disregarded for our analysis. Until the first mass transfer, the components of both models evolve almost identically, as is expected for models with mainly the same input physics (see Chapter 2). The wind mass loss in the ComBinE model appears to be slightly stronger overall than in the MESA model, but not to such a degree that the evolution would be affected. Once the primary models fill their respective Roche lobes, differences start to appear regarding the amount of mass lost from the primary and accretion to the secondary because ComBinE uses a different mass transfer prescription than MESA. In the ComBinE model, the entire envelope of the primary is removed. In contrast, the primary model in MESA retains a part of its envelope, as seen in Fig. 3.20. In fact, the total primary mass in the ComBinE model after mass transfer is roughly equal to the core mass of the primary in the MESA model, with the remaining envelope accounting for the difference in mass. The secondary can accrete more mass in the ComBinE model than in the MESA model. This is because the model of the secondary star starts out non-rotating in ComBinE, while the stellar models are rotating such that they are tidally synchronized in MESA. The mass accretion is limited by the spin-up to critical rotation due to angular momentum accretion in both models, which means that more mass is accreted in the ComBinE model until the secondary reaches critical rotation.
After mass transfer has concluded, the components continue their evolution separately in both the ComBinE and MESA models until the primary depletes helium. At this point, even though the treatment of the supernova is the same in both models, they end up with significantly different

[3] For why this happens to the envelope binding energy, see Kruckow et al. (2016)
[4] In ComBinE, burning stages are faster than in MESA. Source: private communication with Christoph Schürmann

outcomes regarding final mass and orbital period (see Figs 3.19 and 3.16, respectively). The primary of the MESA model loses more mass than the primary in the ComBinE model, as most of the remaining envelope is ejected. Still, the former ends up with a black hole that is $5.4\,M_\odot$ more massive than the latter because the primary in the MESA model can increase its helium core mass through hydrogen layer burning after the Roche-lobe overflow, as can be seen in Fig. 3.21, which shows nuclear energy generation outside the core after ~ 4 Myrs. The primary in the ComBinE model on the other hand consists only of the helium core after mass transfer. The impact of the supernova kick in our models on the orbital period is strongly dependent on the amount of ejected mass (Eq. 2.5). Due to the aforementioned differences, the outcome is significantly altered even when using the same kick velocity and angles, resulting in a post-supernova orbital period in the ComBinE model that is more than 2.7 times larger than the value in the MESA model. It is interesting however, that such a significant deviation still leads to a similar evolutionary outcome for both binary models.

The time from the primary supernova to the next binary interaction is handled slightly differently in the MESA model than the ComBinE model. In the latter, recircularization takes place over a period of time, until about 4.4 Myrs after its zero-age main sequence (see Fig. 3.16 after the first supernova). Afterwards, the orbit widens again through wind mass loss. In the MESA model on the other hand, recircularization is implemented as an instantaneous effect and orbit widening from wind mass loss is neglected. Instead, the model for the secondary star is evolved as a single star after the primary supernova, keeping the orbital period constant until the next binary interaction.

Compared to the differences in orbital period from the supernova kick, the orbit widening from wind mass loss is small, its lack in our MESA model should therefore not be a significant problem. The evolution of the secondary itself is remarkably similar however (compare in the HR diagram, Fig. 3.15), as the difference in mass is small with $0.7\,M_\odot$.

In both the ComBinE and the MESA model, the secondary rapidly expands when hydrogen is depleted, filling their respective Roche lobes and initiating the common envelope evolution. As the orbital period of the ComBinE model is ~ 4.7 times that of the MESA model, its secondary needs to expand further until the Roche lobe is filled (Fig. 3.17), which results in a later onset of mass transfer relative to its evolutionary status. The binding energy of the envelope decreases with stellar radius (Eq. 1.4), making the ejection of the common envelope easier. The envelope binding energy of both secondary models over time is shown in Fig. 3.18. It is calculated differently in the ComBinE model than the MESA model. While ComBinE uses an estimate for the envelope structure parameter λ and the (α,λ)-formalism to calculate the binding energy, in MESA it is directly calculated from the stellar structure according to Eq. 1.4 for each model step, which should be a more accurate prediction for how strongly the envelope is bound in a star. During most of their evolution, the envelope of the secondary ComBinE model is significantly more strongly bound than that of the MESA model. At the point of common envelope onset however, their respective binding energies have almost the same value, leading to an envelope ejection in both cases.

As a consequence of the differences in binding energy over time, the MESA model predicts that a possible common envelope can be more easily ejected than predicted by ComBinE, especially as the absolute value of the binding energy decreases further for the later onset in ComBinE. This is backed up by our investigation into the effect of the primary supernova kick velocity in our models (see Table 3.2), which showed that in the MESA model a wider range of post-supernova orbital periods can lead to a successful common envelope evolution than in the equivalent ComBinE model. In fact, at the post-supernova orbital period from the MESA model, the binary would not survive the common envelope according to ComBinE.

For the MESA model however, our results from Section 3.3.2 suggest that all but the closest common envelopes might survive the process and eventually merge in a gravitational wave event. Consequently, the population synthesis of ComBinE might underestimate the contribution of the

binary evolution channel via common envelope evolution to gravitational wave merger progenitors, a possibility which will be discussed further in Chapter 4.
In the ComBinE model, the mass of the ejected envelope is $15.4\,M_\odot$ out of a total secondary mass of $36.0\,M_\odot$ compared to $19.1\,M_\odot$ out of $38.2\,M_\odot$ in the MESA model, which constitutes 50% of the total mass in the latter case (see Fig. 3.19). Both models use the same criterion for the core-envelope boundary, defined as the point with a hydrogen mass fraction of $X = 0.1$. As the absolute value of the binding energy increases with envelope mass (Eq. 1.4), the aforementioned result that the envelope of the secondary in the MESA model is less strongly bound than that of the ComBinE model has to stem from the contribution of the internal energy (see Section 2 on how the codes calculate it). In particular, the envelopes of the stellar models used in ComBinE seem to be more compact than the ones created with MESA.
The orbital period after common envelope is similar in both models, with the ComBinE value being slightly larger, which is ultimately the cause of the gravitational wave merger happening later in that model. The difference stems mainly from the larger pre-common envelope orbital period in the ComBinE model and the accumulated differences in component masses. As the orbital period after common envelope is always very small (< 0.19 days for our models with different supernova kicks, see Table 3.2), the differences are not particularly relevant to the overall outcome, even when the values resulting from the largest kick velocities are almost four times the values for the slower kicks.
After the common envelope phase is resolved, the ComBinE and MESA models continue with different assumptions for the core of the secondary. ComBinE uses the same underlying helium stellar models regardless of metallicity, while we approximated the secondary with a helium zero-age main sequence model at SMC metallicity for MESA. The ComBinE helium stellar models do not expand at masses $\gtrsim 20\,M_\odot$ (see fig. 5 in Kruckow et al. (2018)), meaning the secondary model with $20.6\,M_\odot$ is affected by this phenomenon as seen in Fig. 3.24. Consequently, the components do not interact anymore after common envelope ejection and the secondary concludes its evolution like a single helium star. The MESA model on the other hand does expand, filling its Roche lobe 0.1 Myr after common envelope ejection and triggering stable mass transfer once more. The main effect of this Roche-lobe overflow is a further decrease in the mass of the secondary. The model for the primary black hole is predicted to accrete $0.1\,M_\odot$ of the transferred mass before it spins up to critical rotation. This indicates that the complications of modelling binary evolution for systems including common envelope evolution have to be considered until the end of the component lifetimes. Helium depletion of the secondary ends the modelling in MESA, and it can not be ruled out that another mass transfer might be initiated. As the Roche-lobe overflow during helium burning has no substantial consequences for the evolutionary outcome beyond reduction in the secondary's mass however, another mass transfer would not be expected to change more than that either.
The second supernova removes more mass from the secondary in the ComBinE model than it does in the MESA model due to the mass transfer in the latter case removing most of the helium envelope from the model of the secondary. As a consequence, the effect of using the same supernova kick parameters is once again different for both models, with the MESA model ending up with a closer and more eccentric orbit. This leads to a faster gravitational wave merger compared to the ComBinE model, with 7.7 Myrs and 16 Myrs since the zero-age main sequence respectively, which is however not a significant difference when compared to the Hubble time of 10 Gyrs. Both models conform to the expectations for merger times from our results in Section 3.1.
While the final masses of both components in the MESA model deviate from those predicted by the ComBinE model, they are consistent with the final masses as measured for GW151012 (Figs. 3.10 - 3.12). Due to the large uncertainties in measurement, it is impossible to conclude whether one model fits the data better than the other.

Overall, it is surprising how the many differences between the binary evolution of the ComBinE and MESA model still lead to such a similar result in the end. As we only study one model each in detail, this result might at least partially be a coincidence. Trying to reproduce a different detailed MESA model from this evolutionary channel in ComBinE might not be as successful, as evidenced by our investigations into the effect of supernova kicks on the outcome of the common envelope phase, which showed that ComBinE might be underestimating the percentage of systems that can eject the common envelope. This will be a point of discussion in the next chapter.

3.5 Summary

In our section using population synthesis with ComBinE, we found that for our chosen initial masses of $60\,M_\odot$ and $40\,M_\odot$ several evolutionary paths from the binary evolution channel are predicted to contribute to observable observable gravitational wave mergers. In particular, the standard formation channel including common envelope evolution ('RLO+CE') seems to be the most promising overall. While supernova kicks can destroy many systems, they can also produce conditions allowing the binary to survive until a gravitational wave merger. At least for kick velocities up to $200\,km\,s^{-1}$, there is always at least one evolutionary path that can produce gravitational wave mergers within the Hubble time for our models.
Using the information from ComBinE, we created a detailed binary model using MESA from the zero-age main sequence to the gravitational wave merger. We showed that the MESA model agrees with the ComBinE result that binary systems undergoing common envelope evolution might be progenitors for gravitational wave mergers. In particular, this evolutionary path constitutes a possible binary progenitor for GW151012.
We also found that ComBinE might underestimate the contribution of this formation channel to gravitational wave mergers, based on when it is possible to eject the common envelope.

Chapter 4

Discussion and Outlook

4.1 Discussion

The results of the previous chapter support the hypothesis that binary evolution via a common envelope is a viable formation channel for producing binary black holes that eventually merge in a gravitational wave event. Both ComBinE and MESA agree that the common envelope can be successfully ejected in our example model and that the black holes merge within the Hubble time (see Table 3.1). The results from the MESA model indicate that the rapid binary code ComBinE might underestimate the contribution of the standard formation channel to gravitational wave events (Section 3.3.2, Fig. 3.18).

Several possible evolutionary paths for our mass pair of $60M_{\odot}$ and $40M_{\odot}$ emerged in the ComBinE models, depending on the initial orbital period (Fig. 3.1). From these, the standard formation channel (called 'RLO+CE' in the results) seems to be the most promising candidate for gravitational wave progenitors. All of the surviving models following this pathway merge within the Hubble time, which is the requirement for a gravitational wave event to be observable today. The majority of all models merging within the Hubble time also evolve along the standard formation channel (Fig. 3.3). While all evolutionary paths from the ComBinE results are dependent on supernova kicks in some way, this evolutionary path is possible for the largest range of supernova kick parameters. It is also the only pathway that can still produce mergers without a supernova kick at all (see Section 3.1.1 , Figs. 3.4 - 3.9).

The results from the MESA model further support the viability of this formation channel, as both ComBinE and MESA models produce the expected outcome, which is a gravitational wave merger fitting the data from GW151012. Despite the deviations between the models in the different evolutionary stages, their overall prediction is remarkably similar (Section 3.4). That two significantly different methods support the viability of the standard formation channel is further evidence for the hypothesis that binaries evolving along this channel contribute to gravitational wave events.

If indeed common envelope ejection is easier than ComBinE predicts, gravitational wave merger rates from this formation channel should be higher than population synthesis studies with ComBinE predict. Depending on the ejection efficiency of the common envelope, binaries might survive common envelope evolution soon after the secondaries (mass donors) reach the evolutionary stage where any mass transfer would be unstable (see Fig. 3.26 , Table 3.2).

The other three evolutionary paths with models merging within the Hubble time present in the ComBinE results can not be ruled out completely and they might contribute to gravitational wave mergers as well. All but the initially closest models fit the observational data available for GW151012 (Figs. 3.10 - 3.12). These other evolutionary paths are more dependent on the impact of supernova kicks on the orbital period. The pathways consist of models undergoing

two stable Roche-lobe overflows, a common envelope evolution without interaction prior to the first supernova, and those undergoing a stable Roche-lobe overflow without interacting before the first supernova. If any of these formation channels contribute to gravitational wave mergers, their contribution is likely to be smaller than that of the standard formation channel, at least for the investigated masses (Section 3.1.1) However, their appearance as gravitational wave progenitors in the ComBinE models mean that in general, massive binaries could end in gravitational wave mergers more easily than previously thought.

4.1.1 Limitations and uncertainties

All of the results in this thesis and their implications depend on our parameter choices and the validity of the assumptions regarding stellar physics. Unfortunately, many of the processes involved in the binary evolution of massive stars contain major uncertainties.
As explained in Chapter 1 , the evolution of even single massive stars is poorly understood. Each parameter choice in the physics underlying the ComBinE and MESA models carries uncertainties. How internal mixing is treated in a model has significant consequences on the binary's evolution, particularly mixing from convection, including convective overshooting, and semiconvection. In this thesis, we worked with values for these processes previously used in the literature (e.g. Brott et al. (2011), Marchant et al. (2016), Kruckow et al. (2018)). As parameter values are constrained further through future observations and through comparisons to model predictions, current models might need to be adapted. For now, they represent educated guesses at minimum. This fact doesn't diminish the validity of the models created for this thesis, the incomplete knowledge about internal processes needs to be acknowledged, however. Comparison to predictions from models using other parameter values is also limited.
The interactions of binaries present us with even more ambiguities regarding the evolution of massive stars. One major uncertainty lies in the treatment of the supernova in the stellar evolution codes, both in the amount of fallback a black hole receives at formation (Eq. 2.4) and regarding the supernova kick (Eq. 2.5). While observations of pulsars provide us with constraints for the supernova kicks during neutron star formation (Hobbs et al. (2005)), they are largely unknown for black hole formation. Estimates range from no kicks (e.g. Nelemans et al. (1999)) to several hundreds $\mathrm{km\,s^{-1}}$ (e.g. Janka (2013)). One the one hand, if black holes do not receive kicks at all during their formation, the only remaining evolutionary path to a gravitational wave merger within a Hubble time for our chosen parameter ranges in the ComBinE models would be the standard formation channel ('RLO+CE'). On the other hand, if supernova kicks were always in the range $\gtrsim 180\,\mathrm{km\,s^{-1}}$, the 'RLO+RLO' channel would be the only one remaining, because the initially wide binaries of the standard formation channel would be disrupted (see Fig. 3.4 for the first supernova and Fig. 3.7 for the second). Predictions become even more difficult when taking kick angles into account (Figs. 3.5 and 3.6 show kick angles from the first supernova, Figs. 3.8 and 3.9 from the second).
How much mass is ejected and how much falls back onto the black hole is another complication of the black hole formation process. The ComBinE models use a simplified method that is the same for all black holes (see Section 2.1.3) and we adopt the same treatment for our MESA model. The uncertainty in this process affects the orbital period and eccentricity after the supernova. In the ComBinE models, the ejection of the common envelope is highly sensitive to the post-supernova orbital period. The MESA model is more robust regarding changes in the onset of the common envelope (comparison in Table 3.2), indicating that uncertainties in the fallback might not be one of the central issues.
The second major set of uncertainties is related to the common envelope evolution itself. Whether a common envelope is created or the mass transfer remains stable depends on the chosen criteria for mass transfer stability. In this thesis, neither Darwin instabilities nor critical mass ratios (see

Section 2.1.3) played a role, because we looked at relatively wide binaries with a specific pair of initial masses. Therefore, the criterion relevant for the instability of a mass transfer is whether the envelope of the mass donor is sufficiently convective, with 10% of the stellar mass contained in a convective region of the envelope. In the MESA model, the envelope is not completely convective yet when the common envelope evolution sets in (see Fig. 3.22 : common envelope evolution onset right at transition from radiative to convective). In particular, the earliest possible common envelope ejection according to the results in Section 3.3.2 occurs when the envelope barely exceeds the adopted criterion for the amount of envelope mass that needs to be convective[1]. Therefore, any change regarding this criterion would impact the results of that section significantly.

Another vital criterion in the outcome of a common envelope evolution is the location of the boundary between the core and the envelope. Ivanova et al. (2013) discuss the difficulty of determining this boundary and different methods for doing so in detail. Using the same definition for the ComBinE models and the MESA model maintains their comparability. The chosen boundary, the point where the hydrogen mass fraction is $X = 0.1$ (Dewi & Tauris (2000)), has also been used previously in literature (e.g. Kruckow et al. (2018)), therefore our results can be directly compared to their binary models as well.

Ivanova et al. (2013) also discuss other potential modifications to the energy budget during the common envelope evolution that might aid or hinder the envelope ejection. Until the entire common envelope evolution can be modelled self-consistently, the question whether orbital energy is the only significant contribution to the ejection of the envelop may remain unsolved. The ejection efficiency parameter represents what percentage of the released orbital energy can actually be converted into kinetic energy for the envelope. In this thesis, a value of $\alpha_{\mathrm{CE}} = 0.5$ was used. For now, it is uncertain whether this is a realistic value and whether using one value for all binaries undergoing common envelope evolution is an adequate assumption. It is reasonable to assume $\alpha_{\mathrm{CE}} < 1$, because some energy will be lost to radiation. Since the envelope needs to escape the binary, $\alpha_{\mathrm{CE}} = 1$ would imply not only perfect energy conversion, the process also would need to be fine-tuned, such that no excess energy is deposited into the envelope.

Kruckow et al. (2018) discussed the consequences of changing the value of the ejection efficiency parameter in their ComBinE models, which our models are based on. As expected, increasing the value would increase the amount of systems that can survive the common envelope evolution, while decreasing it would do the opposite. In our MESA model however, the ejection of the envelope is easier (Figs. 3.18 and 3.26). Increasing α_{CE} would effectively lead to an earlier envelope ejection, which would be associated with a larger orbital period at the formation of the second black hole. Consequently, the gravitational wave merger would happen later (Eq. 2.8). The MESA model is still sensitive to a lower value for the ejection efficiency parameter. From our results in Fig. 3.26, we can see at which orbital periods at the common envelope onset the model would still predict an ejection of the envelope for a given value of α_{CE}.

Parameter choices in this thesis limit how much the results can be generalized. The results show possible outcomes for one mass pair at one metallicity. Only their initial orbital and the supernova kicks were varied in the ComBinE models (Table 2.2). As explained in Chapter 1, the low metallicity and relatively low masses of the stellar models mean that wind mass loss is not an essential factor in their evolution. At larger masses, envelope inflation also becomes a significant complication (Köhler et al. (2015)). Therefore, we expect the detailed stellar models for much more massive stars to be significantly different, and so should the outcomes of their binary evolution. For similar and lower initial masses however, the results could be more comparable, as long as the stars are still massive enough to form black holes. Progenitors of neutron star binaries might still form through the standard formation channel present in our results as well, but their modelling needs to follow different principles, as detailed in Kruckow et al. (2018). They also investigated the effect of

[1] based on the output from MESA, see code available at `https://github.com/k-rauth/master-thesis`

metallicity on the formation of black hole binaries through the standard formation channel. They found that gravitational wave merger rates are decreased for higher metallicities. Therefore, we also expect that a similar effect would be seen for MESA models with higher metallicities.
The limitations presented in this section are a problem for all models of binary star evolution, and do not diminish our results. On the contrary, our models fill a void in previous research, as previously no detailed models existed that followed a binary from zero-age main sequence to the binary black hole formation and the subsequent gravitational wave merger. Even with the uncertainties discussed here, we found a model for a binary that could be a progenitor for GW151012 with both of the methods used in this thesis.

4.1.2 Comparison to previous studies and observations

As our ComBinE models are restricted to one mass pair, they do not represent a population synthesis study from which expected merger rates could be deduced. However, they are based on the work by Kruckow et al. (2018), who calculated expected merger density rates for binary black hole mergers between $6.01 \times 10^{-1}\,\mathrm{Gpc^{-3}yr^{-1}}$ at galactic metallicity, and $16.8\,\mathrm{Gpc^{-3}yr^{-1}}$ at the lowest studied metallicity, that of the dwarf galaxy I Zwicky 18. Abbott et al. (2019) released an update for the empirical merger rate density of binary black holes, which was determined to be $9.7 - 101\,\mathrm{Gpc^{-3}yr^{-1}}$. For low metallicities, the results from Kruckow et al. (2018) could fit the observations, but the value corresponds to the low end of the empirical range. The comparison to our MESA model showed that the contribution of binaries that survive a common envelope evolution might be underestimated in ComBinE (Section 3.4). This would correspond to a larger expected merger rate density.
A study by Stevenson et al. (2017) investigated potential progenitors for GW151012 with another rapid binary evolution code. Their results also support the hypothesis that the progenitors of this event could have evolved through the standard formation channel. Interestingly, their result for the median final mass ratio is $q \approx 0.5$ at SMC metallicity, which is also the final mass ratio in our MESA model. The initial total mass range at SMC metallicity is constrained to $95 \lesssim M\,/\,\mathrm{M_\odot} \lesssim 125$, which is consistent with our chosen initial system mass of $100\,\mathrm{M_\odot}$.
A recent study using MESA models starting at the BH + main sequence star phase (Marchant et al. (2021)), proposed that most binary black hole progenitors might not undergo and survive the common envelope evolution at all, instead favoring a second stable Roche-lobe overflow. This formation channel corresponds to the 'RLO+RLO' path in our ComBinE results (see Section 3.1). Our models indeed indicate that progenitors undergoing two stable Roche-lobe overflows might be almost as numerous as the ones undergoing a common envelope evolution after their first mass transfer (Fig. 3.3). Our result is predicated on supernova kicks from black hole formation reaching values up to $200\,\mathrm{km\,s^{-1}}$ (see Section 3.1.1). The result of Marchant et al. (2021) is limited to a single donor mass at $30\,\mathrm{M_\odot}$, while the donor mass at the onset of the common envelope evolution in our MESA model is $38.2\,\mathrm{M_\odot}$ (see Table 3.1). Both models use similar metallicities. This discrepancy hints that results from a model at one can not easily be generalized toward predictions for outcomes at other masses. However, our MESA model is not directly comparable to theirs because of different choices in the convection and semiconvection parameters, which can alter models of stellar evolution drastically.
Another recent study analyzed observed galactic Wolf-Rayet stars with a companion black hole (Sen et al. (2021)), and concluded that the observations of black hole + O star binaries do not require large kicks at black hole formation to be explained. Therefore, their results further support the validity of the standard formation channel, which would not be viable if supernova kicks were too large, based on our results in Section 3.1.1.

Previous studies have also proposed alternative formation channels for progenitors of gravitational wave events. The chemically homogeneous evolution channel for binaries (Marchant et al. (2016)) proposes that the components start out close together, with initial orbital periods of less than two days. Tidal interactions induce strong mixing in the stars, causing them to avoid the post-main sequence expansion massive stars normally experience. This formation channel predicts final mass ratios close to $q = 1$ and is only possible for chirp masses $\mathcal{M} \gtrsim 20\,\mathrm{M}_\odot$. GW151012, with $q \gtrsim 0.24$, has a maximum chirp mass of $17.3\,\mathrm{M}_\odot$, therefore the chemically homogeneous formation channel can not explain this event.
In the dynamical formation channel, the black holes meet after their individual formation in a dense stellar environment (e.g. Rodriguez et al. (2015)). Due to the little amount of information we have on GW151012, this formation channel can not be ruled out. The value of the effective in-spiral spin parameter X_{eff} for GW151012 is close to zero (see Table 2.1), which according to Farr et al. (2017) is consistent with a dynamical formation history. They present the hypothesis that a history of mass transfer results in aligned spins of the black holes, which would show up as a positive value for X_{eff}. However, supernova kicks might destroy this alignment again. Since our progenitor models are constructed with a supernova kick, $X_{\mathrm{eff}} \approx 0$ is not a problem regarding the validity of our results. While we can not rule out the dynamical formation channel for GW151012, Abbott et al. (2019) present two gravitational wave events with $X_{\mathrm{eff}} > 0$. Therefore, even if the hypothesis is correct, the dynamical formation channel can not explain every gravitational wave merger, and other explanations for merging black hole binaries are needed.

4.2 Outlook

The results of this thesis represent one step in deepening our understanding of possible binary star progenitors for gravitational wave events. They are possibly the first attempt at using a detailed stellar evolution code for a model of the standard formation channel for gravitational wave progenitors, with binary evolution from the zero-age main sequence to the binary black hole stage. Due to the aforementioned limitations, more studies for different initial masses and metallicities will be needed in order to make general predictions. The method we developed offers a possibility to investigate the common envelope formation channel with detailed stellar evolution models, without requiring the capability to self-consistently model the common envelope evolution itself. To investigate a larger grid of massive binary star models at different metallicities, existing binary grids could be combined with the methods demonstrated in this work.
Another future work could be a detailed investigation into the other three evolutionary paths predicted to produce gravitational wave mergers within the Hubble time present in our ComBinE results (Section 3.1). The 'RLO+RLO' channel might be of interest in particular, as detailed stellar evolution codes can solve Roche-lobe overflows and this channel is predicted to produce the second most gravitational wave mergers in the Hubble time (Fig. 3.3).
By adapting our method to the different evolutionary paths, it would be possible to get a detailed model that follows massive binary stars from zero-age main sequence to the binary black hole stage using a maximum of two MESA runs. The evolutionary path with a common envelope evolution as the only binary interaction ('none+CE') could even be investigated by using single star evolution for the secondary until the onset of common envelope evolution. Should future studies also come to the conclusion that binary survivors of the common envelope evolution merge within the Hubble time in general (as seen in Fig. 3.1), a detailed binary evolution following the envelope ejection might not even be necessary.
Overall, the implications from our results are fascinating and could form the basis of future studies into the details of the standard formation channel for gravitational wave progenitors.

Chapter 5

Conclusion

This thesis aimed to find a binary star model as a progenitor for the gravitational wave event GW151012, using the rapid binary code ComBinE and the detailed stellar evolution code MESA, version 10398. In GW151012, two black holes with masses of $23.3\,M_\odot$ and $13.6\,M_\odot$ merged. We created a large number of binary star models with ComBinE (Section 3.1). By restricting ourselves to a specific pair of initial masses, $60\,M_\odot$ and $40\,M_\odot$ at SMC metallicity, we could study the consequences of variations in the initial orbital period and of supernova kicks in detail.
From these models, we identified the so-called standard formation channel, in which a binary undergoes common envelope evolution, to be the most likely candidate for producing the gravitational wave event (Section 3.2). In addition, our results featured three more possible binary formation channels for producing gravitational wave mergers within the Hubble time (Fig. 3.1). The Hubble time approximates the age of the universe, which means that any gravitational wave mergers observable today must have merged faster than this.
We compared the range of initial orbital periods that could produce the gravitational wave merger through the standard formation channel to a grid of existing MESA binary models created by Chen Wang. An initial orbital period for which the MESA model predicted survival until the onset of common envelope evolution was chosen. MESA can not simulate the impact of a supernova kick on a binary or the common envelope evolution. We created a method to predict the outcome of each event from the MESA model, which enabled the start of second binary MESA model that simulates the remaining evolution if the common envelope can be ejected (Section 3.3).
Both the ComBinE model and the comparable MESA model predicted a successful ejection of the common envelope and a subsequent gravitational wave merger within the Hubble time. The MESA model also predicted the common envelope ejection to be significantly easier than expected from the ComBinE models. This result indicates that ComBinE might underestimate the contribution of binaries evolving through the standard formation channel to the gravitational wave merger rates (Section 3.4).
Previous studies have used rapid binary codes to find models for gravitational wave progenitors. This thesis represents a novel approach towards this goal by using detailed stellar models, possibly for the first time. While not a solution to the uncertainties regarding processes like the common envelope evolution (Section 4.1.1), our results point towards the developed method being a promising new way to investigate potential progenitors of gravitational wave mergers.
Because the significantly different methods used in this work both agree in their outcome, we conclude that the standard formation channel is a viable pathway for the evolution of the progenitors of GW151012. In general, these results increase our confidence that binaries of massive stars contribute to observable gravitational wave events.

Bibliography

Abbott, B. P. et al. (2019), 'GWTC-1: A Gravitational-Wave Transient Catalog of Compact Binary Mergers Observed by LIGO and Virgo during the First and Second Observing Runs', *Phys. Rev. X* **9**(3), 031040.

Belczynski, K., Holz, D. E., Bulik, T. & O'Shaughnessy, R. (2016), 'The first gravitational-wave source from the isolated evolution of two stars in the 40-100 solar mass range', *Nature* **534**(7608), 512–515.

Böhm-Vitense, E. (1958), 'Über die Wasserstoffkonvektionszone in Sternen verschiedener Effektivtemperaturen und Leuchtkräfte. Mit 5 Textabbildungen', *Z. Astrophys.* **46**, 108.

Brott, I., de Mink, S. E., Cantiello, M., Langer, N., de Koter, A., Evans, C. J., Hunter, I., Trundle, C. & Vink, J. S. (2011), 'Rotating massive main-sequence stars. I. Grids of evolutionary models and isochrones', *Astronomy and Astrophysics* **530**, A115.

Darwin, G. H. (1879), 'The Determination of the Secular Effects of Tidal Friction by a Graphical Method', *Proceedings of the Royal Society of London Series I* **29**, 168–181.

de Mink, S. E., Cantiello, M., Langer, N., Pols, O. R., Brott, I. & Yoon, S. C. (2009), 'Rotational mixing in massive binaries. Detached short-period systems', *Astronomy and Astrophysics* **497**(1), 243–253.

Detmers, R. G., Langer, N., Podsiadlowski, P. & Izzard, R. G. (2008), 'Gamma-ray bursts from tidally spun-up Wolf-Rayet stars?', *Astronomy and Astrophysics* **484**(3), 831–839.

Dewi, J. D. M. & Tauris, T. M. (2000), 'On the energy equation and efficiency parameter of the common envelope evolution', *Astronomy and Astrophysics* **360**, 1043–1051.

Eggleton, P. P. (1983), 'Approximations to the radii of Roche lobes', *ApJ* **268**, 368.

Farr, W. M., Stevenson, S., Miller, M. C., Mandel, I., Farr, B. & Vecchio, A. (2017), 'Distinguishing spin-aligned and isotropic black hole populations with gravitational waves', *Nature* **548**(7667), 426–429.

Hamann, W. R., Koesterke, L. & Wessolowski, U. (1995), 'Spectral analyses of the Galactic Wolf-Rayet stars: hydrogen-helium abundances and improved stellar parameters for the WN class', *Astronomy and Astrophysics* **299**, 151.

Han, Z., Podsiadlowski, P. & Eggleton, P. P. (1995), 'The formation of bipolar planetary nebulae and close white dwarf binaries', *Monthly Notices of the Royal Astronomical Society* **272**(4), 800–820.

Heger, A. & Langer, N. (2000), 'Presupernova Evolution of Rotating Massive Stars. II. Evolution of the Surface Properties', *The Astrophysical Journal* **544**(2), 1016–1035.

Heger, A., Langer, N. & Woosley, S. E. (2000), 'Presupernova Evolution of Rotating Massive Stars. I. Numerical Method and Evolution of the Internal Stellar Structure', *ApJ* **528**, 368–396.

Hills, J. G. (1983), 'The effects of sudden mass loss and a random kick velocity produced in a supernova explosion on the dynamics of a binary star of arbitrary orbital eccentricity. Applications to X-ray binaries and to the binarypulsars.', *The Astrophysical Journal* **267**, 322–333.

Hobbs, G., Lorimer, D. R., Lyne, A. G. & Kramer, M. (2005), 'A statistical study of 233 pulsar proper motions', *Monthly Notices of the Royal Astronomical Society* **360**(3), 974–992.

Iglesias, C. A. & Rogers, F. J. (1996), 'Updated Opal Opacities', *The Astrophysical Journal* **464**, 943.

Ivanova, N., Justham, S., Chen, X., De Marco, O., Fryer, C. L., Gaburov, E., Ge, H., Glebbeek, E., Han, Z., Li, X. D., Lu, G., Marsh, T., Podsiadlowski, P., Potter, A., Soker, N., Taam, R., Tauris, T. M., van den Heuvel, E. P. J. & Webbink, R. F. (2013), 'Common envelope evolution: where we stand and how we can move forward', *Astronomy and Astrophysics Review* **21**, 59.

Janka, H.-T. (2013), 'Natal kicks of stellar mass black holes by asymmetric mass ejection in fallback supernovae', *Monthly Notices of the Royal Astronomical Society* **434**(2), 1355–1361.

Kippenhahn, R., Weigert, A. & Weiss, A. (2012), *Stellar Structure and Evolution*.

Köhler, K., Langer, N., de Koter, A., de Mink, S. E., Crowther, P. A., Evans, C. J., Gräfener, G., Sana, H., Sanyal, D., Schneider, F. R. N. & Vink, J. S. (2015), 'The evolution of rotating very massive stars with LMC composition', *Astronomy and Astrophysics* **573**, A71.

Kruckow, M. U., Tauris, T. M., Langer, N., Kramer, M. & Izzard, R. G. (2018), 'Progenitors of gravitational wave mergers: binary evolution with the stellar grid-based code combine', *Monthly Notices of the Royal Astronomical Society* **481**(2), 1908–1949.
URL: *http://dx.doi.org/10.1093/mnras/sty2190*

Kruckow, M. U., Tauris, T. M., Langer, N., Szécsi, D., Marchant, P. & Podsiadlowski, P. (2016), 'Common-envelope ejection in massive binary stars. Implications for the progenitors of GW150914 and GW151226', *A&A* **596**, A58.

Langer, N. (1991), 'Evolution of massive stars in the Large Magellanic Cloud - Models with semiconvection', *A&A* **252**, 669–688.

Langer, N. (2012), 'Presupernova Evolution of Massive Single and Binary Stars', *Annual Review of Astronomy and Astrophysics* **50**, 107–164.

Langer, N., Fricke, K. J. & Sugimoto, D. (1983), 'Semiconvective diffusion and energy transport', *Astronomy and Astrophysics* **126**(1), 207.

Langer, N., Schürmann, C., Stoll, K., Marchant, P., Lennon, D. J., Mahy, L., de Mink, S. E., Quast, M., Riedel, W., Sana, H., Schneider, P., Schootemeijer, A., Wang, C., Almeida, L. A., Bestenlehner, J. M., Bodensteiner, J., Castro, N., Clark, S., Crowther, P. A., Dufton, P., Evans, C. J., Fossati, L., Gräfener, G., Grassitelli, L., Grin, N., Hastings, B., Herrero, A., de Koter, A., Menon, A., Patrick, L., Puls, J., Renzo, M., Sander, A. A. C., Schneider, F. R. N., Sen, K., Shenar, T., Simón-Días, S., Tauris, T. M., Tramper, F., Vink, J. S. & Xu, X. T. (2020), 'Properties of OB star-black hole systems derived from detailed binary evolution models', *Astronomy and Astrophysics* **638**, A39.

Marchant, P., Langer, N., Podsiadlowski, P., Tauris, T. M. & Moriya, T. J. (2016), 'A new route towards merging massive black holes', *Astronomy and Astrophysics* **588**, A50.

Marchant, P., Pappas, K. M. W., Gallegos-Garcia, M., Berry, C. P. L., Taam, R. E., Kalogera, V. & Podsiadlowski, P. (2021), 'The role of mass transfer and common envelope evolution in the formation of merging binary black holes', *Astronomy and Astrophysics* **650**, A107.

Nelemans, G., Tauris, T. M. & van den Heuvel, E. P. J. (1999), 'Constraints on mass ejection in black hole formation derived from black hole X-ray binaries', *Astronomy and Astrophysics* **352**, L87–L90.

Nieuwenhuijzen, H. & de Jager, C. (1990), 'Parametrization of stellar rates of mass loss as functions of the fundamental stellar parameters M, L, and R.', *Astronomy and Astrophysics* **231**, 134–136.

Paxton, B., Bildsten, L., Dotter, A., Herwig, F., Lesaffre, P. & Timmes, F. (2011), 'Modules for Experiments in Stellar Astrophysics (MESA)', *ApJS* **192**, 3.

Paxton, B., Cantiello, M., Arras, P., Bildsten, L., Brown, E. F., Dotter, A., Mankovich, C., Montgomery, M. H., Stello, D., Timmes, F. X. & Townsend, R. (2013), 'Modules for Experiments in Stellar Astrophysics (MESA): Planets, Oscillations, Rotation, and Massive Stars', *ApJS* **208**, 4.

Paxton, B., Marchant, P., Schwab, J., Bauer, E. B., Bildsten, L., Cantiello, M., Dessart, L., Farmer, R., Hu, H., Langer, N., Townsend, R. H. D., Townsley, D. M. & Timmes, F. X. (2015), 'Modules for Experiments in Stellar Astrophysics (MESA): Binaries, Pulsations, and Explosions', *ApJS* **220**, 15.

Paxton, B., Schwab, J., Bauer, E. B., Bildsten, L., Blinnikov, S., Duffell, P., Farmer, R., Goldberg, J. A., Marchant, P., Sorokina, E., Thoul, A., Townsend, R. H. D. & Timmes, F. X. (2017), 'Modules for Experiments in Stellar Astrophysics (MESA): Convective Boundaries, Element Diffusion, and Massive Star Explosions', *ArXiv e-prints* .

Peters, P. C. (1964), 'Gravitational Radiation and the Motion of Two Point Masses', *Physical Review* **136**(4B), 1224–1232.

Podsiadlowski, P. (2001), 'Evolution of Binary and Multiple Star Systems; A Meeting in Celebration of Peter Eggleton's 60th Birthday', **229**.

Rodriguez, C. L., Morscher, M., Pattabiraman, B., Chatterjee, S., Haster, C.-J. & Rasio, F. A. (2015), 'Binary black hole mergers from globular clusters: Implications for advanced ligo', *Phys. Rev. Lett.* **115**, 051101.
URL: *https://link.aps.org/doi/10.1103/PhysRevLett.115.051101*

Sanyal, D., Grassitelli, L., Langer, N. & Bestenlehner, J. M. (2015), 'Massive main-sequence stars evolving at the Eddington limit', *Astronomy and Astrophysics* **580**, A20.

Sen, K., Xu, X. T., Langer, N., El Mellah, I., Schurmann, C. & Quast, M. (2021), 'X-ray emission from BH+O star binaries expected to descend from the observed galactic WR+O binaries', *arXiv e-prints* p. arXiv:2106.01395.

Stevenson, S., Vigna-Gómez, A., Mandel, I., Barrett, J. W., Neijssel, C. J., Perkins, D. & de Mink, S. E. (2017), 'Formation of the first three gravitational-wave observations through isolated binary evolution', *Nature Communications* **8**, 14906.

Sutantyo, W. (1974), 'On the tidal evolution of massive X-ray binaries.', *Astronomy and Astrophysics* **35**, 251–257.

Tassoul, J.-L. (1978), *Theory of rotating stars*.

Tauris, T. M. & Bailes, M. (1996), 'The origin of millisecond pulsar velocities.', *Astronomy and Astrophysics* **315**, 432–444.

Tauris, T. M. & Dewi, J. D. M. (2001), 'Research Note On the binding energy parameter of common envelope evolution. Dependency on the definition of the stellar core boundary during spiral-in', *Astronomy and Astrophysics* **369**, 170–173.

Tauris, T. M., Langer, N. & Podsiadlowski, P. (2015), 'Ultra-stripped supernovae: progenitors and fate', *Monthly Notices of the Royal Astronomical Society* **451**(2), 2123–2144.

Tauris, T. M. & Takens, R. J. (1998), 'Runaway velocities of stellar components originating from disrupted binaries via asymmetric supernova explosions', *Astronomy and Astrophysics* **330**, 1047–1059.

Tauris, T. M. & van den Heuvel, E. P. J. (2006), *Formation and evolution of compact stellar X-ray sources*, Vol. 39, pp. 623–665.

Vink, J. S., de Koter, A. & Lamers, H. J. G. L. M. (2001), 'Mass-loss predictions for O and B stars as a function of metallicity', *Astronomy and Astrophysics* **369**, 574–588.

Voss, R. & Tauris, T. M. (2003), 'Galactic distribution of merging neutron stars and black holes - prospects for short gamma-ray burst progenitors and LIGO/VIRGO', *Monthly Notices of the Royal Astronomical Society* **342**(4), 1169–1184.

Wang, C., Langer, N., Schootemeijer, A., Castro, N., Adscheid, S., Marchant, P. & Hastings, B. (2020), 'Effects of Close Binary Evolution on the Main-sequence Morphology of Young Star Clusters', *The Astrophysical Journal* **888**(1), L12.

Wellstein, S., Langer, N. & Braun, H. (2001), 'Formation of contact in massive close binaries', *A&A* **369**, 939–959.

Yoon, S. C. & Langer, N. (2005), 'Evolution of rapidly rotating metal-poor massive stars towards gamma-ray bursts', *Astronomy and Astrophysics* **443**(2), 643–648.

Yoon, S. C., Langer, N. & Norman, C. (2006), 'Single star progenitors of long gamma-ray bursts', *Nuovo Cimento B Serie* **121**(12), 1631–1632.

Appendix

A.1 Special notes

- Footnote in Section 3.1 : In the version of ComBinE used for this thesis, a bug caused a crash after creating a certain number of models. Troubleshooting of the code led to the conclusion that the validity of our results should not be affected.
- Table 3.2 : Regarding the predicted CE merger for a supernova kick velocity of $0\,\mathrm{km\,s^{-1}}$. This is the case when using the ComBinE recipe, which still applies an eccentricity due to mass lost from the binary system. The effects without a kick are significantly different from a small kick, which is why $0\,\mathrm{km\,s^{-1}}$ and $20\,\mathrm{km\,s^{-1}}$ predict a CE merger, while $10\,\mathrm{km\,s^{-1}}$ predicts a stable RLO. When removing the impact of the supernova entirely from the code for the MESA model, the result is similar to the one with a $50\,\mathrm{km\,s^{-1}}$ kick, as evidenced by very similar orbital period pre- and post-supernova for that model in Fig. 3.16.
- Footnote in Section 3.2.1: Why does the HRD (Fig. 3.15) show more time steps for the ComBinE model components than other plots? Answer: HRD shows evolution of individual components, based directly on interpolation from the single star models. These do not contain the corrections from binary interactions, which are very important for mass, radius, etc. The ComBinE file including these corrections contains fewer time steps for the binary model.

A.2 Additional figures

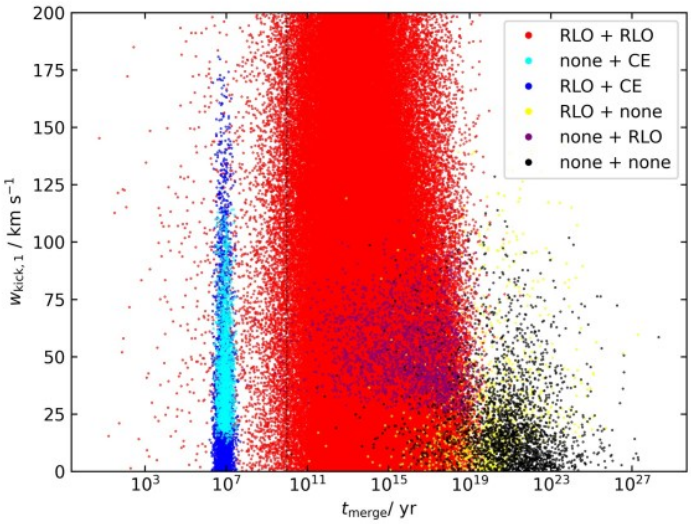

Figure A.1: Kick velocities from the first supernova for the same ComBinE models as in Fig. 3.1 versus their merger times. For each binary system, kick velocity was randomly chosen between $0 - 200$ km/s. As before, the major interaction possibilities are color-coded (see legend). The dashed line indicates a merger time of 10^{10} yrs.

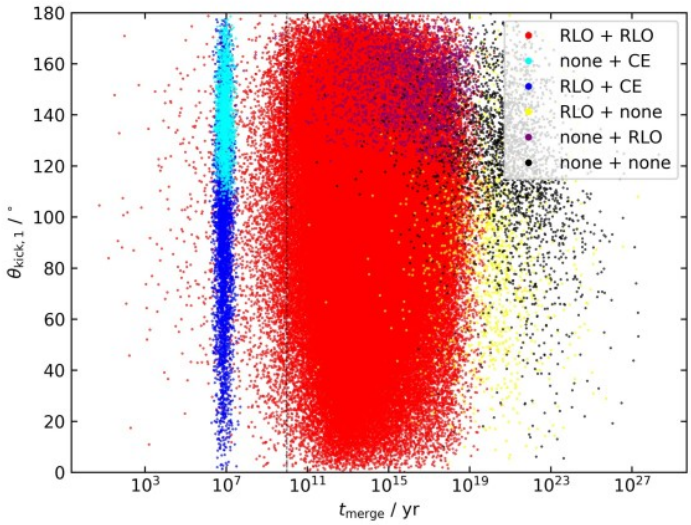

Figure A.2: Kick angles θ from the first SN for the ComBinE models from Fig. 3.1 versus their merger time. For each binary system, θ was randomly chosen between $0 - 180°$. Each of the six possibilities for major interactions leading to a GW merger are color-coded (see legend). The dashed line indicates a merger time of 10^{10} yrs.

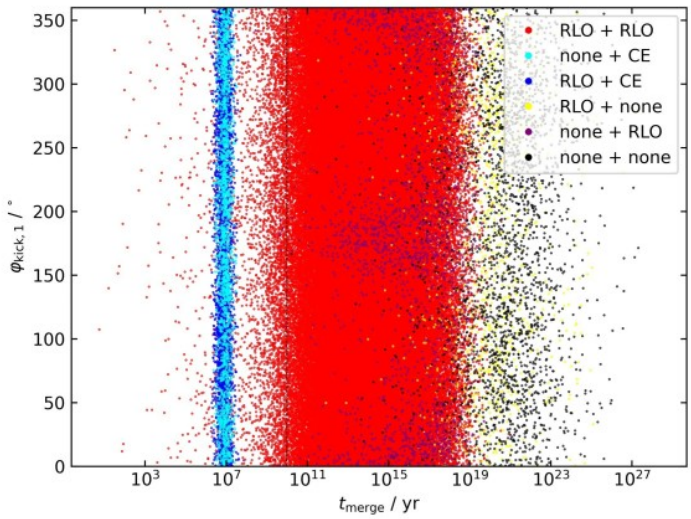

Figure A.3: Kick angles φ from the first SN for the ComBinE models from Fig. 3.1 versus their merger time. φ was randomly chosen between $0 - 360°$ for each binary model. As before, major interactions are color-coded (see legend) and the dashed line shows a merger time of 10^{10} yrs.

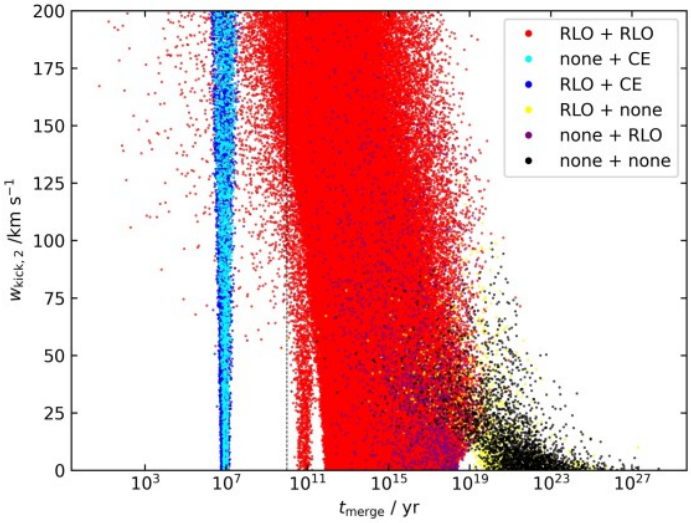

Figure A.4: Kick velocities from the second SN for for the same ComBinE models as before (Fig. 3.1) versus their merger times. For each binary system, kick velocity was randomly chosen between $0 - 200$ km/s, independent of first kick (Fig. A.1). As before, the major interaction possibilities are color-coded (see legend). The dashed line indicates a merger time of 10^{10} yrs.

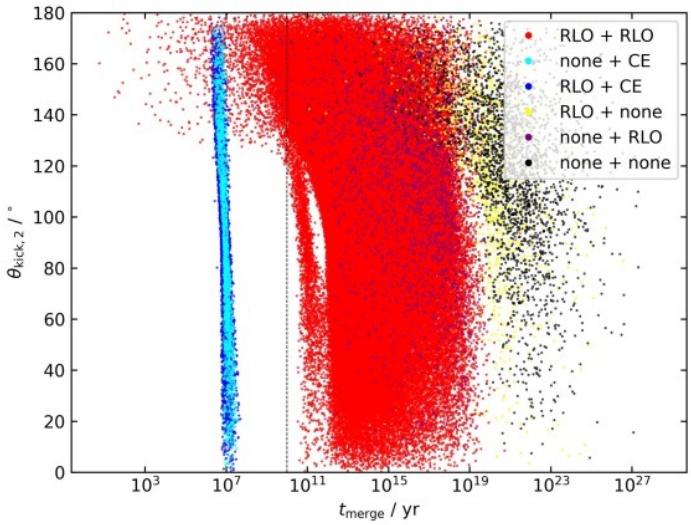

Figure A.5: Kick angles θ from the second SN for the ComBinE models from Fig. 3.1 versus their merger time. For each binary system, θ was randomly chosen between $0 - 180°$. Each of the six possibilities for major interactions leading to a GW merger are color-coded (see legend). The dashed line indicates a merger time of 10^{10} yrs.

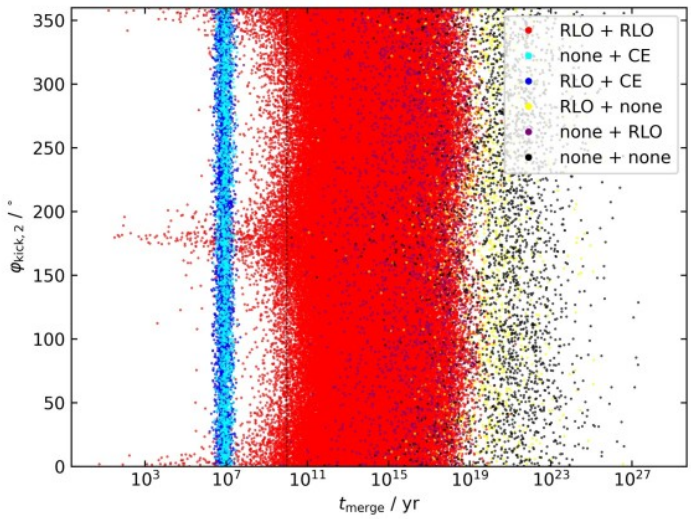

Figure A.6: Kick angles φ from the second SN for the ComBinE models from Fig. 3.1 versus their merger time. φ was randomly chosen between $0 - 360°$ for each binary model. As before, major interactions are color-coded (see legend) and the dashed line shows a merger time of 10^{10} yrs.

List of Figures

List of Tables